STUDIECENTRUM VOOR KERNENERGIE
CENTRE D'ETUDE DE L'ENERGIE NUCLEAIRE

EXTERNAL REPORT
SCK•CEN-ER-237
13/Kva/P-72

Solute Transport in Boom Clay

Katrijn Vandersteen, Matej Gedeon, Mieke De Craen

SCK•CEN contract: CO-90-08-2214-00
NIRAS/ONDRAF contract: CCHO 2009-0940000
Research Plan Geosynthesis

October, 2013

SCK•CEN
Boeretang 200
BE-2400 Mol
Belgium

PAS

ISO 9001 CERTIFIED VINÇOTTE

Solute Transport in Boom Clay

Katrijn Vandersteen, Matej Gedeon, Mieke De Craen

SCK•CEN contract: CO-90-08-2214-00
NIRAS/ONDRAF contract: CCHO 2009-0940000
Research Plan Geosynthesis

October, 2013
Status: Unclassified
ISSN 1782-2335

SCK•CEN
Boeretang 200
BE-2400 Mol
Belgium

© SCK•CEN
Studiecentrum voor Kernenergie
Centre d’étude de l’énergie Nucléaire
Boeretang 200
BE-2400 Mol
Belgium

Phone +32 14 33 21 11
Fax +32 14 31 50 21

http://www.sckcen.be

Contact:
Knowledge Centre
library@sckcen.be

Abstract

This report compiles and discusses information from various research projects both conducted at SCK•CEN and at other institutes concerning the nature of the transport processes occurring in the Boom Clay in NE-Belgium. These so-called multiple lines of evidence were investigated in order to come to a consistent view on the mechanisms of solute transport in Boom Clay under past and present conditions.

The relevant Boom Clay properties related to solute transport discussed in the report are the porosity and the hydraulic conductivity. The considered elements of the hydrogeological context that have influence on the mechanisms of solute transport are the hydraulic gradient and the flow/Darcy velocity, from which the Péclet number was calculated, indicating the dominant transport mechanism in the Boom Clay. Another independent line of evidence describing the main transport mechanism in Boom Clay was given by the modelling interpretation of a large scale *in situ* experiment (Weetjens *et al*., 2011) and of natural tracer profiles in the Boom Clay (Mazurek *et al*., 2009, 2011). Finally, the influence of possible preferential flow paths (fractures and specific layers containing septarian concretions) on solute transport in Boom Clay was described.

It was found that - with the current knowledge - these multiple lines of evidence all indicate diffusion–dominated transport through Boom Clay under past and present conditions or, at least, they do not give any evidence of the occurrence of other than diffusion-dominated transport. However, some unresolved issues still remain.

Table of Contents

1. Introduction and Objectives

In Belgium, the Boom Clay is considered as a potential host rock for the geological disposal of radioactive waste. An essential characteristic of a suitable host rock is the limited water-flow through the host rock (ONDRAF/NIRAS, 2009 a-b-c). In this framework, all known transport processes in the Boom Clay are described in this report.

Geoscientific evidence for these transport processes is given through a compilation of information from a variety of research projects that have been conducted both at SCK•CEN and at other institutes. Geo-scientific evidence comes from various research projects in which the host rock properties and hydrogeological context of the Boom Clay are studied, diffusion/advection experiments and associated transport calculations are done and/or preferential flow is described, in order to come to a consistent view on the mechanisms of solute transport in Boom Clay.

A schematic overview of these multiple lines of evidence is given in Figure 1. The relevant Boom Clay properties related to solute transport are the porosity and the hydraulic conductivity. The elements of the hydrogeological context that have influence on the mechanisms of solute transport are the hydraulic gradient and the flow/Darcy velocity, from which the Péclet number can be calculated, indicating the dominant transport mechanism in the Boom Clay. Another independent line of evidence describing the main transport mechanism in Boom Clay was given by the modelling interpretation of a large scale *in situ* experiment (Weetjens *et al*., 2011) and of natural tracer profiles in the Boom Clay (Mazurek *et al*., 2009, 2011). Finally, the influence of possible preferential flow paths (fractures and specific layers containing septarian concretions) on solute transport in Boom Clay is described.

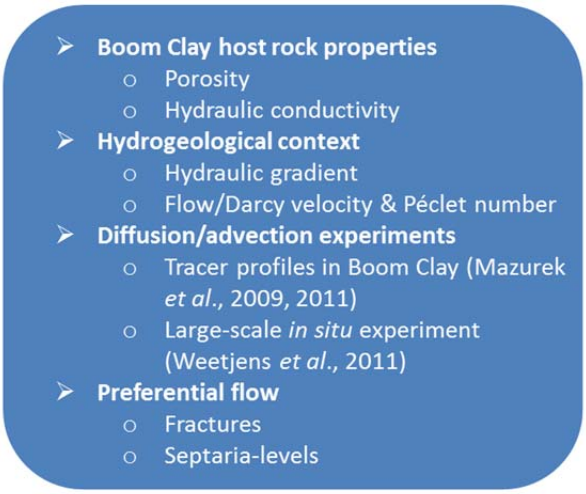

Figure 1: Multiple lines of evidence derived from various research disciplines to come to a consistent view on the mechanisms of solute transport in Boom Clay.

The objective of this report is to describe the relevant transport processes in the Boom Clay in NE-Belgium for the past and the present situation, using experimental evidence. The report gives a phenomenological description of solute transport in Boom Clay.

The Boom Clay is present throughout the Campine area, located in the provinces of Antwerp and Limburg, in NE-Belgium (Figure 2).

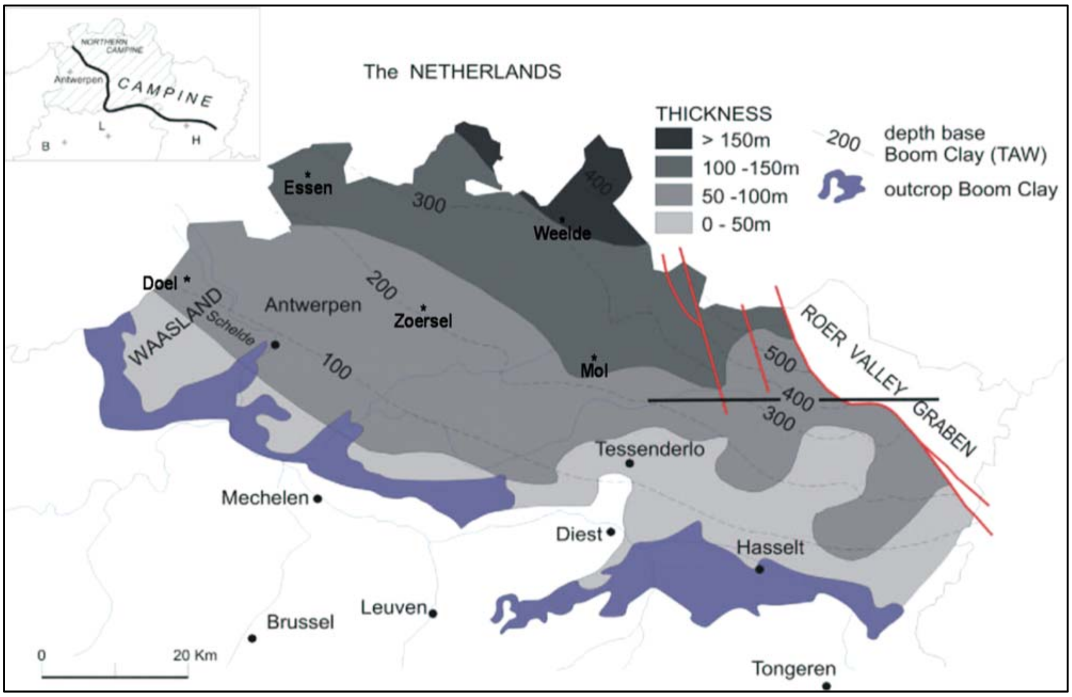

Figure 2: Outcrop and subcrop of the Boom Clay in Belgium, also showing depth to base relative to sea level and thickness (from SAFIR 2, ONDRAF/NIRAS, 2001).

2. Transport processes

The main known transport processes through low-permeable material (like the Boom Clay) are diffusion, dispersion and advection. Besides these three processes, other transport processes exist, like thermal and density driven flow. These other processes are often considered to be of minor importance (e.g. Mazurek *et al*., 2011).

2.1. Advection, dispersion and diffusion

Transport by advection is defined as transport of solutes by flowing groundwater (Domenico and Schwartz, 1998). Contaminants transported by advection are travelling in the same direction and at the same rate as the average linear velocity of the groundwater. Accordingly, the velocity of advective transport is described by the Darcy equation as follows:

$$\boldsymbol{v} = -\frac{\boldsymbol{K}}{\boldsymbol{n_e}}\frac{\boldsymbol{\partial h}}{\boldsymbol{l}} \qquad \text{Equation 1}$$

Where v is the linear or pore velocity of groundwater [m/s], K is the hydraulic conductivity [m/s], n_e is the effective porosity [-] and $\partial h/l$ [-] is the hydraulic gradient. The effective porosity is defined as the percentage of interconnected pore space.

Transport by mechanical dispersion is defined as mixing caused by local variations in velocity around a mean velocity of flow (Domenico and Schwartz, 1998). Mechanical dispersion is an advective process. Variability in the direction and rate of transport is caused by non-idealities in the porous medium. Although in reality mechanical dispersion and (chemical) diffusion are different processes, mathematically, transport by mechanical dispersion is described in the same way as transport by diffusion. In reality, transport by diffusion and mechanical dispersion cannot be separated during groundwater flow. Therefore, the two terms are lumped into the hydrodynamic dispersion coefficient as follows:

$$\boldsymbol{D} = \boldsymbol{D'} + \boldsymbol{D_d^*} \qquad \text{Equation 2}$$

Where D is the hydrodynamic dispersion tensor [m^2/s], $D' = \alpha v$ is the mechanical dispersion tensor [m^2/s], α is the dynamic dispersivity [m], v is average linear or pore groundwater flow velocity [m/s] and D_d^* is the bulk diffusion coefficient [m^2/s].

Transport by diffusion is defined as the process by which solutes dissolved in groundwater move from areas of higher concentration to areas of lower concentration (Domenico and Schwartz, 1998). Fick's Law describes how chemical mass flux is proportional to the gradient in concentration. In case of diffusion in a fluid phase of a porous sediment, Fick's Law becomes:

$$\boldsymbol{J} = -D_d^* n\, grad(C) \qquad \text{Equation 3}$$

Where J is a chemical mass flux [moles/m^2s], C is concentration [mol/m^3], n is porosity [-], and $\boldsymbol{D_d^*}$ is the bulk diffusion coefficient accounting for the effects of tortuosity [m^2/s]. Since diffusion is independent of groundwater flow, it is possible for solutes to move through a porous medium by diffusion, even though the groundwater is not flowing (Fetter, 2001).

For systems with fluid motion, mass transport can be due to advection and diffusion. This combined flux can be described mathematically by combining the advective flux in equation 1 and the diffusive flux in equation 3, resulting in the advection-diffusion equation, of which the one-dimensional form is as follows:

$$D_d^* \frac{\partial^2 C}{\partial x^2} - v_x \frac{\partial C}{\partial x} = \frac{\partial C}{\partial t}$$ Equation 4

The first term on the left describes mass transport by diffusion and the second describes mass transport by advection. When taking into account mechanical dispersion, the bulk diffusion coefficient D_d^* is replaced by the coefficient of hydrodynamic dispersion *D*, and equation 4 transforms into the advection-dispersion equation.

In dimensionless form, equation 4 becomes (Domenico and Schwartz, 1998):

$$\nabla^{+2} C^+ - \frac{vL}{D_d^*} \nabla^+ C^+ = \frac{L^2}{t_e D_d^*} \frac{\partial C^+}{\partial t^+}$$ Equation 5

where $C^+ = C/C_e$ is a dimensionless concentration, C_e is some characteristic concentration, and the superscript + indicates a dimensionless quantity. The dimensionless quantity vL/D_d^* is the Péclet number for mass transport with *L* as some characteristic length.

At high flow velocities, transport may be advection-dispersion dominated. At low flow velocities, transport may be diffusion dominated since transport by advection may be even slower than the very slow process of transport by diffusion. Transport by advection is often neglected in low-permeable media based on a Péclet number criterion, relating the effectiveness of mass transport by advection to the effectiveness of mass transport by either dispersion or diffusion (Fetter, 1999). Usually, diffusion is considered as the dominant transport mechanism for Péclet numbers smaller than one. Unfortunately, up to ten different definitions of the Péclet number can easily be found in literature and for a given particular case these different definitions lead to very diverse Péclet numbers. Hence, deciding to neglect advection based only on a Péclet number smaller than one seems not justified for every existing Péclet number definition (Huysmans and Dassargues, 2005; Huysmans, 2006).

2.2. Other transport processes

This section presents the so-called coupled or off-diagonal transport processes and summarizes the conclusions of some relevant studies on this subject, related to their importance for radioactive waste disposal in clay formations.

Synthesized by Horseman *et al.* (1996) in the framework of radioactive waste disposal, a coupled transport process (or Onsagerian coupled flux) is a "flow" of any kind (e.g. fluid, heat, electrical current and solute), which is driven by gradients of a potential not usually associated with that flow, or what we could call a non-conjugate force. Table 1 represents the matrix for direct and coupled phenomena for different transport processes (after Soler, 2001).

Some coupled transport phenomena (thermal and chemical osmosis, hyperfiltration, cross-diffusion, thermal diffusion, thermal filtration, Dufour effect) may play an important role in fluid, solute and heat transport in clay-rich formations. Rocks containing large proportions of compacted clays may act as semipermeable membranes due to the existence of ionic double layers on the clay surfaces. Unfortunately, the physical parameters ruling most of the Onsagerian processes are poorly known.

Table 1. Onsager matrix – matrix of direct (diagonal) and coupled (off-diagonal) transport phenomena (de Marsily, 1986; Horseman *et al*., 1996). (Table from Soler, 2001).

Flux J	Potential gradient X			
	Temperature	Hydraulic	Chemical	Electrical
Heat	Thermal conduction	Thermal filtration	Dufour effect	Peltier effect
Fluid	Thermal osmosis	Advection	Chemical osmosis	Electrical osmosis
Solute	Thermal diffusion or Soret effect	Hyperfiltration	Diffusion	Electrophoresis
Current	Seebeck or Thompson effect	Rouss effect	Diffusion and membrane potential	Electrical conduction

Soler (2001) provided estimates of the magnitudes of the fluxes associated with coupled transport phenomena in Opalinus Clay. The main conclusion arising from this study is that coupled phenomena will only have a very minor impact on radionuclide transport in the Opalinus Clay, at least under the conditions at the expected time of waste canister failure (times equal to or greater than 1000 years). For shorter times, i.e., shortly after the emplacement of the waste canisters in the repository, temperature gradients will be larger and will also be changing rapidly with time near the repository (steady state cannot be assumed; desaturation and resaturation of the rock near the repository may occur). The effect of coupled phenomena during this transient phase is still open to question.

Garavito *et al*., (2007) conducted an *in situ* chemical osmosis experiment in the Boom Clay at the HADES URF in order to investigate the osmotically induced pressure increase. The experimental results obtained *in situ* confirm the occurrence of non-hydraulic flow phenomena (chemical osmosis) in a low-permeability plastic formation such as the Boom Clay. The osmotic efficiency of Boom Clay is high under undisturbed chemical conditions, but rapidly decreases when the dissolved salts concentration increases.

Mazurek *et al*., (2011) state that in clay-rich rocks, additional processes like chemical osmosis (e.g. Soler, 2001) and hyperfiltration can affect water flow and solute transport. These processes affect measured effective diffusion coefficients and may be responsible for overpressures within a clay formation. There is, however, no compelling evidence that they have a major influence on solute transport across large, consolidated clay formations (e.g. Garavito *et al*., 2007).

Based on the studies by Soler (2001) and Garavito *et al*., (2007) it seems that in particular chemico-osmosis (and also thermo-osmosis and thermo-diffusion in case of large temperature gradients) could occur in Boom Clay. However, all the modeling calculations performed in the Boom Clay in the past have been predictive in despite of the fact that they do not take into account those Onsagerian processes (Brassines, 2007).

In conclusion, we can state that with the current knowledge, Onsagerian transport processes are most likely of minor relevance for solute transport in Boom Clay under current conditions.

3. Flow through the Boom Clay

Measurements and different experiments conducted at the Hades underground research facility (URF) and on cored regional boreholes crossing the Boom Clay help to describe the relevant flow processes in the Boom Clay along with the relevant parameters and variables related to flow and transport in Boom Clay. First, the interpretation of profiles of natural tracers in pore waters across the Boom Clay (Mazurek *et al*., 2009, 2011) as well as the modelling of a large-scale *in situ* experiment at the HADES URF (Weetjens *et al*., 2011) will be discussed. Secondly, the hydrogeological host rock properties (porosity and hydraulic conductivity) of the Boom Clay are described, both at the Mol site and regionally. Then, the hydrogeological context is discussed, consisting of a derivation of the hydraulic gradient and the velocity over the Boom Clay both at the Mol site and in NE-Belgium (Campine), resulting in an indicative calculation of Péclet numbers over the Boom Clay. Finally, possible preferential flow through Boom Clay is discussed, i.e. through layers containing septarian carbonate concretions and fractures.

3.1. Experimental evidence of flow processes in Boom Clay

3.1.1 Analysis of natural tracer profiles

A summary of the work done by Mazurek *et al*. (2009, 2011) is presented here, providing strong indication that diffusion is the dominant transport process in pore waters across the Boom Clay. The geochemical evolution of natural tracer profiles in several clay formations including the Boom Clay, both in Mol and in Essen, was studied in the CLAYTRAC project (Mazurek *et al*., 2009, 2011). Based on a careful evaluation of the palaeo-hydrogeological evolution of the area, model scenarios were derived for initial and boundary pore-water compositions (in this case from seawater composition to actual pore water composition), and an attempt was made to numerically reproduce the observed tracer distributions in a consistent way, using transport parameters derived from laboratory or *in situ* tests. A summary of the main results is given in the following paragraphs. Only results from Essen are shown as they deal with the largest variety in tracers. Results from Mol are similar.

In Essen, marine conditions prevailed until about 1.7 Ma ago, when the area emerged from the sea. Fresh-water infiltration has probably occurred since the time of emergence. The underlying Oligocene aquifer crops out ca. 40 km further south. In the Essen borehole, the pore-water salinity and water-isotope signature correspond to a sea-water proportion of 20% mixed with meteoric water. Vertical tracer profiles through the Boom Clay were constructed for anions (Cl^-, Br^-, I^-), stable isotopes (δ^2H, $\delta^{18}O$) and dissolved gases (He). The tracer profiles all show linear patterns (with the exception of $\delta^{18}O$ and δ^2H in the uppermost part of the Boom Clay) that connect the values in the overlying Neogene fresh-water aquifer and the underlying Oligocene aquifer.

The hypothesis that these tracer distributions represent steady-state diffusion profiles was tested by model calculations using realistic scenarios for the palaeo-hydrogeological evolution. Until emergence from the sea, groundwater in both aquifers as well as the pore water in the Boom Clay are assumed to have consisted of sea water with marine anion concentrations and stable-isotope ratios, and this is taken as the initial condition for the model. Because the Neogene aquifer reaches directly to the surface, it is likely that it was flushed by meteoric water rapidly after emergence and has maintained a meteoric signature since then. In the Oligocene aquifer, the salinity evolution since its emergence is less known. For the base case, the assumption of rapid flushing was also used, implying that the current composition is representative of the whole continental period. Alternative assumptions, such as a linear decrease of salinity with time, were also tested. However, the observed linear depth trends of the tracers can only be reproduced by model calculations if the larger part of the salinity loss occurred in the early part of the evolution since emergence.

Model calculations for Cl^-, He and δ^2H at Essen are presented in Figure 3, Figure 4 and Figure 5 respectively. For Cl^-, after a diffusion time of ca. 1.2–1.4 Ma since emergence, the modelled profile (Figure 3) approaches steady state. It is concluded that the observed near-linear profile of Cl^- over the Boom Clay can be well explained by diffusion alone if the diffusion time exceeds 1.4 Ma with present-day Cl^- concentration in the Oligocene aquifer. Analogous results are obtained for Br^- and I^- (not shown).

The He-concentration at the time of emergence is unknown. However, irrespective of the assumed initial value, the He concentrations adjust to the boundary conditions within ≤1 Ma, and the profile reaches steady state rapidly (Figure 4). Even when an unrealistically high initial He concentration of 10^{-2} cm^3 STP/g_{water} is assumed, near-steady state conditions are reached after only ca. 0.8 Ma, mainly because of the high diffusion coefficient for He and the limited thickness of the Boom Clay. Also, *in situ* production contributes little to the He budget, as seen in the small curvature of the steady-state profile.

The profiles of $\delta^{18}O$ and δ^2H across the Boom Clay can be separated into two segments (Figure 5 for δ^2H). Except for the uppermost ca. 20 m, the profiles for both $\delta^{18}O$ and δ^2H are near-linear and could be interpreted as due to steady-state diffusion. In the uppermost 20 m, the linear trend of the δ values is disturbed. The profile shows a pronounced shift towards the higher δ values that are observed in the Neogene aquifer. This shift can be explained by changed conditions in the Neogene aquifer in response to Holocene warming. Independent evidence for this shift is given by Mazurek *et al.*, 2009, using data from Marivoet *et al.*, 2000 and Phillipot *et al.*, 2000. Figure 5 shows that the model reproduces the data well using these combined boundary conditions.

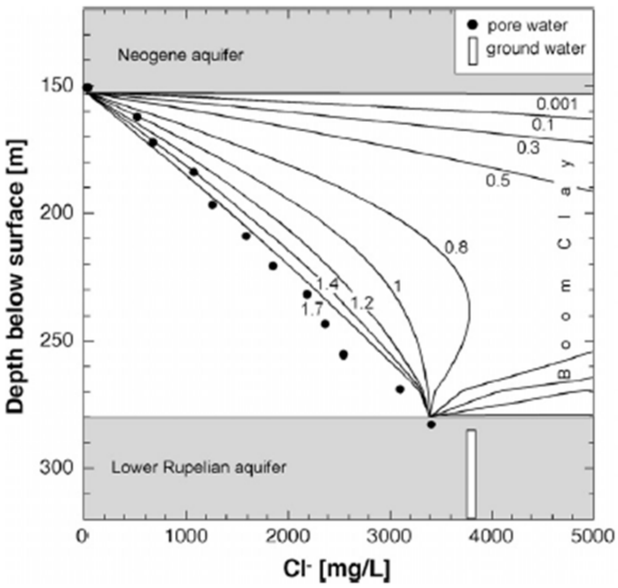

Figure 3: Base-case model for Cl^- at Essen. Only diffusive transport is considered. Numbers adjacent to model curves indicate evolution times in Ma since activation of the aquifers. The Cl^- concentration in the Oligocene aquifer is assumed to be constant and at the current value since emergence of the site at 1.7 Ma. (Mazurek *et al.*, 2011).

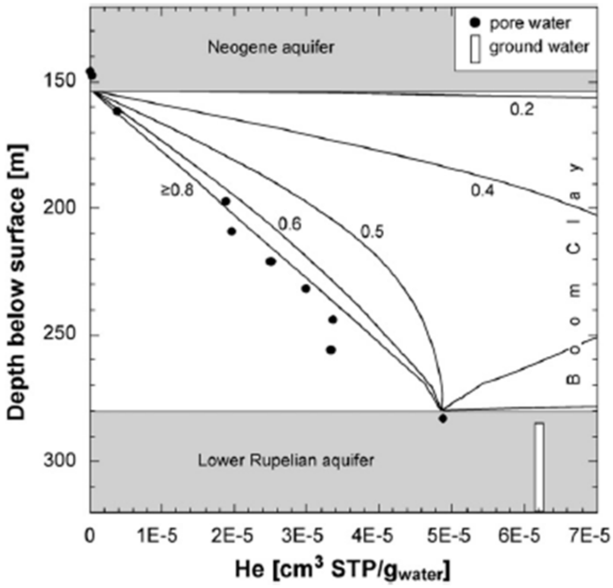

Figure 4. Base-case model for He at Essen, considering diffusion and *in situ* production. Numbers adjacent to model curves indicate evolution times in Ma since activation of the aquifers. The initial He concentration is assumed to be 1×10^{-2} cm^3 STP/g_{water}. (Mazurek *et al.*, 2011).

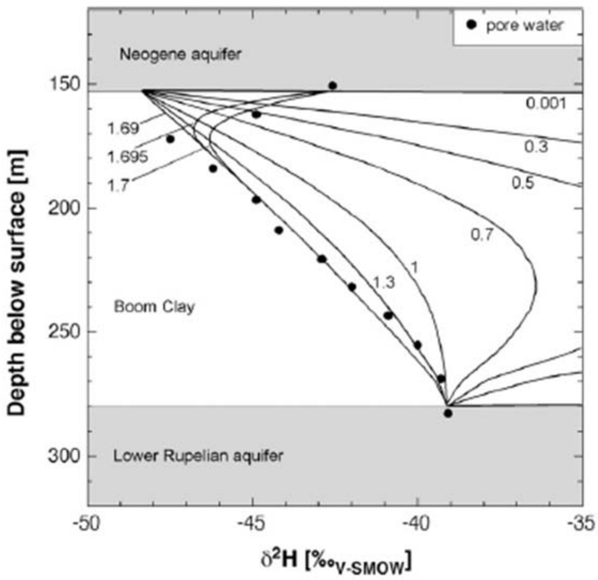

Figure 5. Base case model for δ^2H at Essen (diffusion only). Numbers adjacent to model curves indicate evolution times in Ma since activation of the aquifers. Initial δ^2H = 0 ‰. (Mazurek *et al.*, 2011).

In alternative cases, vertical advection was considered in addition to diffusion. The objective was to test the sensitivity of the model to advective transport. Figure 6 shows that even a small advection velocity of 5×10^{-13} m/s yields a model fit that is less good than diffusion only. Even when considering evolution times >1.7 Ma (which is in conflict with palaeo-hydrogeology), the fit remains less good because a steady-state profile is established with a curvature not seen in the data. The effects of advection on modeled profiles as shown here for Cl^- are analogous for water isotopes and He, and so the same conclusions are reached based on all tracers.

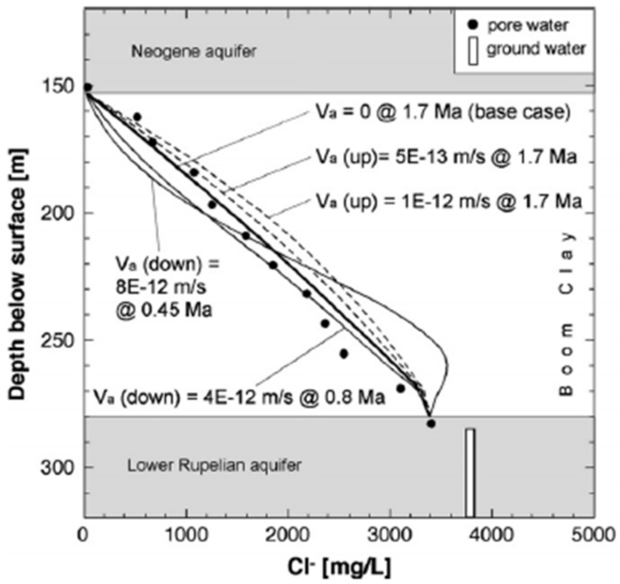

Figure 6. Best fit models for Cl^- at Essen considering diffusion and advection. Thick line: Base case (diffusion only); solid lines: downward advection; broken lines: upward advection. V_a = vertical advection velocity. (Mazurek *et al.*, 2011)

CONCLUSION: For Boom Clay, the shapes of the tracer profiles at Mol and Essen can be explained by diffusion as the dominant transport process, and acting over geological time scales. However, the applied bottom boundary condition for the model, representing rapid flushing of the Oligocene aquifer, has not been supported by other evidence so far and thus remains speculative.

Within the CLAYTRAC project (Mazurek *et al.*, 2009, 2011), similar observations were made for all argillaceaous formations studied, i.e. the Callovo-Oxfordian shale at the site Meuse/Haute Marne (Bure, France), the Couche Silteuse at Marcoule (Gard, France), the Opalinus Clay at Benken, Mont Terri, and Mont Russelin (Switzerland), the Toarcian-Domerian shale at Tournemire (France), the Boom Clay at Mol and Essen (Belgium), and the London Clay at Bradwell (UK). In all tracer profiles, the transport mechanism is dominated by diffusion. In the model cases where advective transport/movement was also considered, the goodness of the model fits to the data could not be improved, suggesting that advective transport is either comparably slow as diffusion, slower, or even absent.

3.1.2 Large-scale in situ experiment at HADES URF

Large scale *in situ* migration experiments - CP1 and Tribicarb-3D (Weetjens *et al.*, 2011) - were designed with the objective to validate the flow and radionuclide transport models and their parameter values in Boom Clay, more specifically to investigate whether transport parameter values determined in laboratory conditions are also valid for larger time and spatial scales. These experiments are situated in the HADES URF.

The principle of these tests consists of installing multi-filter piezometers in which a known quantity of tracer solution is injected in a centrally located filter and the decrease of the tracer concentration in the injection filter and the breakthrough of the tracer at adjacent filters are measured (Figure 7). Tritiated water (HTO) is used to study migration in Boom Clay in both *in situ* tests. In the Tribicarb-3D experiment, bicarbonate is used as an additional tracer. CP1 was started up in 1986 and Tribicarb-3D in 1995. Both experiments are still running.

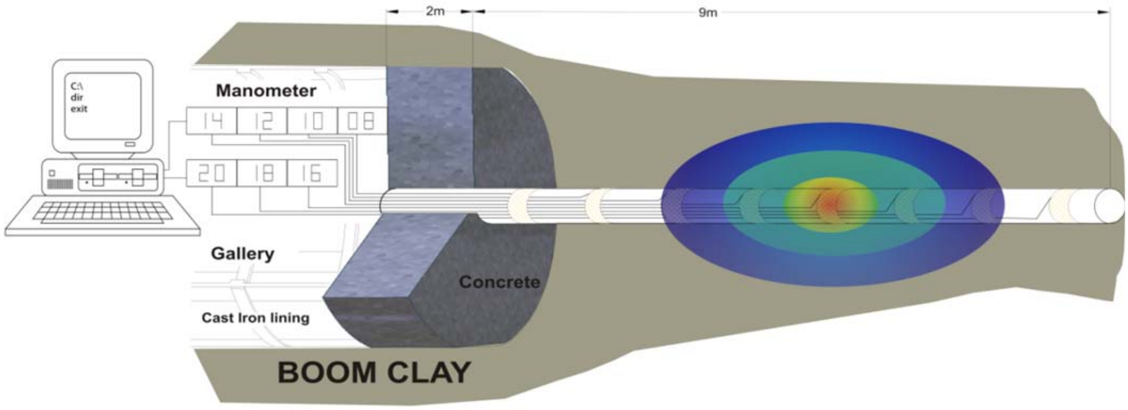

Figure 7: Schematic representation of the CP1 *in situ* migration experiment with HTO (multi-filter piezometer) (Weetjens *et al*., 2011).

The results (diffusion only) are shown for the CP1 experiment in Figure 8. Advection plays a minor role, even for the increased hydraulic gradients in this case (due to the presence of the gallery at atmospheric pressure) compared to a (closed) repository system at *in situ* pressures. Results for the CP1 experiment (diffusion + advection) are given in Figure 9. Refinements of the model were done by introducing the hydraulic evolution of the open gallery together with the resulting Darcy velocity profiles. These refinements led to a small increase in the goodness of fit. The results of the large scale *in situ* migration experiments show the good understanding of the HTO migration in the system and confirm the validity of the transport model for unretarded dissolved species.

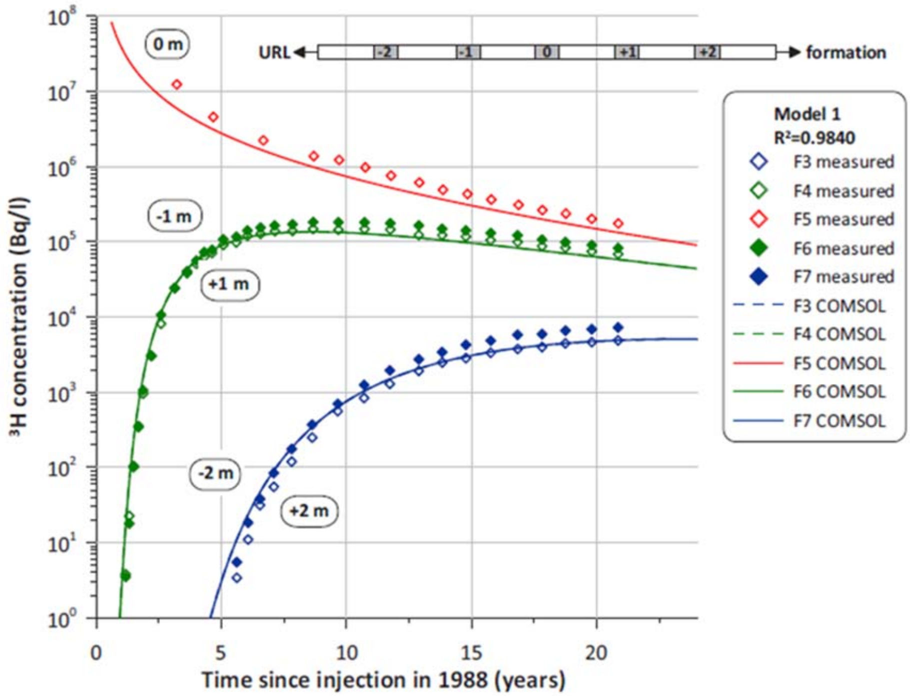

Figure 8. Prediction of the CP1 experiment neglecting advection. Diffusion is isotropic. (Weetjens *et al.*, 2011)

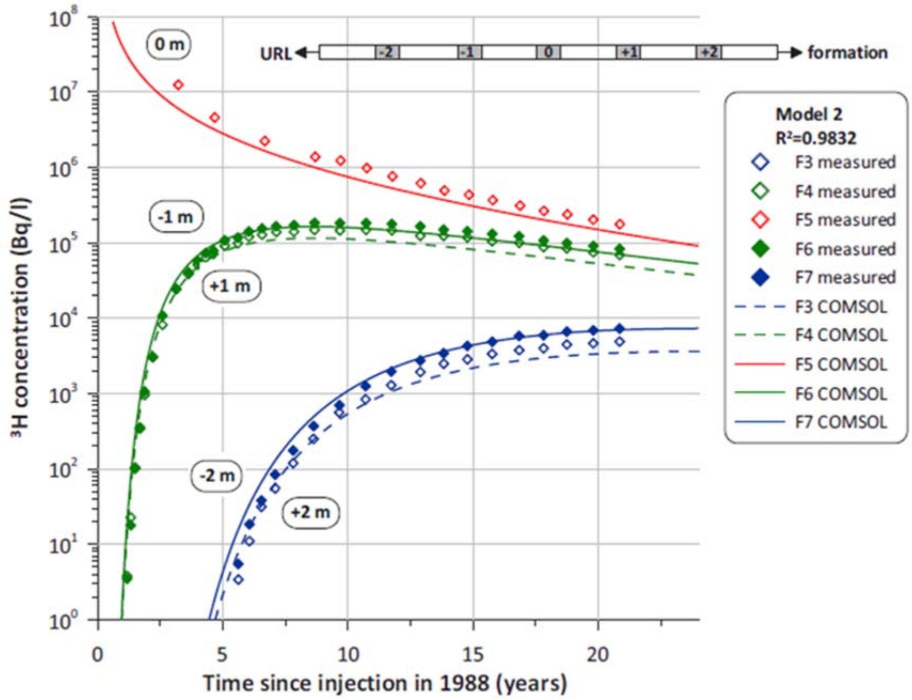

Figure 9. Prediction of the CP1 experiment with constant Darcy velocity. Diffusion is isotropic. (Weetjens *et al.*, 2011).

CONCLUSION: The modelling of the URF experiments (Weetjens *et al.*, 2011) showed that a simplified core model considering only diffusion by using isotropic parameters in the direction of interest is sufficient to give a good correspondence with the observed breakthrough curves at the scale of the experiment.

3.2. Advective transport related Boom Clay host rock properties

The Boom Clay properties relevant for advective solute transport are porosity (effective porosity and pore size) and hydraulic conductivity. These properties allow estimating the rate of advection (pore-water flow velocity) and compare it to the rate of diffusion in the Boom Clay.

3.2.1. Boom Clay porosity

The **effective porosity** (the percent of the total volume of a given mass of soil or rock that consists of interconnected interstices (Jackson, 1997)) of Boom Clay can be determined through radionuclide migration experiments, particularly HTO (tritiated water) diffusion experiments (De Cannière *et al*., 1996). A summary of values of effective porosity (Aertsens *et al*., 2005a, 2005b, 2010) for three boreholes - Mol-1, Doel-2b and Essen-1 - is given in Table 2. The Putte Member in Essen has a higher porosity (0.46) leading to higher average porosity of the Boom Clay Formation in Essen of 0.42 (Aertsens *et al*., 2010). The porosity values of the Boom Clay in the Mol-1 and Doel-2b boreholes were obtained with the same type of experiment and the same model. For Essen-1, another type of experiment and consequently also another model is used, which does not behave well at low Péclet numbers. This might lead to less reliable values for the porosity for HTO. However, the fitted porosities are confirmed by the independently measured water content of an adjacent clay core (Aertsens *et al*., 2010).

Table 2. Diffusion accessible porosity η in three different boreholes, determined from HTO diffusion experiments (Aertsens *et al*., 2005a, Aertsens *et al*., 2005b; Aertsens *et al*., 2010).

Borehole	η [-]
Mol-1	0.37 ± 0.03
Doel-2b	0.39 ± 0.02
Essen-1	0.42 ± 0.05

Pore size and pore size distributions (the volume fractions of the various size ranges of pores in a soil, expressed as percentages of the soil bulk volume (Jackson, 1997)) were measured on three Boom Clay samples taken from the Mol-1 borehole, by means of SEM (manual detection and segmentation of porosities) and mercury-injection porosimetry (MIP) at RWTH in Aachen in the framework of an on-going PhD project (Hemes *et al*., 2012). The three samples are considered to be representative of the observed variations in grain size within the Boom Clay in Mol. The study indicates that **pores smaller than 25-30 nm are most likely to control the interconnectivity of the pore space in fine-grained samples of Boom Clay.**

3.2.2. Boom Clay hydraulic conductivity

The hydraulic conductivity of a porous medium is a measure of its ability to transmit water when submitted to a pressure gradient. Hydraulic conductivity K is defined by Darcy's law, which, for one-dimensional vertical flow, can be written as follows:

$$q = -K\Delta P \qquad \textbf{Equation 6}$$

Where q is the filtration velocity or Darcy flux (discharge per unit area with unit [m/s] and ΔP is the pressure gradient). On the basis of Equation 5, the hydraulic conductivity is defined as the ratio of Darcy's velocity to the applied hydraulic gradient. The dimension of K is the same as that for velocity, that is, length per unit of time [m/s].

Hydraulic conductivity is a function of both properties of the porous medium and properties of the fluid. The important properties relevant to the rock matrix include pore size distribution, pore shape, tortuosity, specific surface and porosity. In relation to the fluid, the important properties include fluid density and fluid viscosity. For a saturated subsurface system like the Boom Clay, the hydraulic conductivity, K, can be expressed as follows (Bear, 1972):

$$K = \frac{\kappa \rho g}{\mu}$$ **Equation 7**

Where κ, the rock intrinsic permeability [m^2] depends only on properties of the solid matrix, and fluid viscosity μ [$kg\ m^{-1}\ s^{-1}$] and fluid density ρ [$kg\ m^{-3}$] represent the properties of the percolating fluid.

The values of saturated hydraulic conductivity K in nature vary within a wide range of several orders of magnitude, depending on the material. Table 3 lists the range of expected K-values for various unconsolidated and consolidated rocks (Bear, 1972).

Table 3: Saturated hydraulic conductivity (*K*) values found in nature typical for fresh water conditions using standard values of viscosity and specific gravity at 20° and 1 atm (modified from Bear, 1972). Gray shading indicates approximately the range of the Boom Clay hydraulic conductivity.

K [m/s]	10^{0}	10^{-1}	10^{-2}	10^{-3}	10^{-4}	10^{-5}	10^{-6}	10^{-7}	10^{-8}	10^{-9}	10^{-10}	10^{-11}	10^{-12}
Relative permeability	Permeable				Semi-permeable				Impermeable				
Aquifer	Good					Poor				None			
Unconsolidated Sand & Gravel	Well Sorted Gravel		Well Sorted Sand or Sand & Gravel			Very Fine Sand, Silt, Loess, Loam							
Unconsolidated Clay & Organic					Peat		Layered Clay			Fat / Unweathered Clay			
Consolidated Rocks	Highly Fractured Rocks				Oil Reservoir Rocks			Fresh Sandstone		Fresh Limestone, Dolomite		Fresh Granite	

When analyzing the hydraulic conductivity data for the Boom Formation, several aspects should be taken into account:

- The generally small **representative volume** of the laboratory tests (sample size) produces hydraulic conductivity data for individual sub-layers of the Boom Clay, whereby the lithology varies from clay, clayey silt to silty- and even sandy clay (Wemaere *et al*., 2002). The difference in these estimates is therefore not related to the uncertainty in the hydraulic conductivity estimation (measurement error) but to the formation heterogeneity;

- The **anisotropy** of the Boom Clay is a scale dependent parameter. Several scales are identified in this context. At the sample scale (small representative volume), intrinsic anisotropy can be measured if samples are taken parallel or perpendicular to the bedding. At the formation scale, the effect of hydraulic conductivities of the individual layers is superposed and the anisotropy value is significantly higher, since the lowest K values have the highest weight in calculating the representative vertical K, however the largest K values receive the highest weight in calculating the representative horizontal K;

- The **lithostratigraphic** division of the Boom Clay is based on its lithological characteristics and has only limited implication on the hydraulic conductivity zoning. The hydraulic conductivity is dependent on the lithology of the individual sub-layers in the Boom Clay;

- The Boom Clay **self-sealing** capacity was shown by the HADES URF Experiments, whereby it was proven that the swelling clay minerals and the visco-elasto-plastic behaviour of the Boom Clay seals fissures under saturated conditions and normal geo-mechanical stress (Bernier *et al*., 2007). Based on these experimental results and the assumption of laterally homogeneous deposition, the existence of fissures that can result in a larger regional value of hydraulic conductivity of the (saturated) Boom Clay is highly improbable. This will be further explained in section 3.4.

The Boom Clay hydraulic conductivity is a key parameter determining water flow through the disposal system. Various sources of information are available concerning the Boom Clay hydraulic conductivity. The hydraulic properties of the Boom Clay at the Mol site have been studied for more than 30 years in the framework of the research program on deep geological disposal of radioactive waste. Both laboratory and *in situ* experiments, carried out on different scales ranging from centimeters to several meters, yielded consistent values of hydraulic conductivity of the Boom Clay. Furthermore, the vertical and regional variability of the Boom Clay hydraulic conductivity has been investigated using several regionally distributed core-drilled boreholes. All results are summarized in Yu *et al*. (2011, 2013). An overview is given below.

<u>Measurement methods</u>
Throughout the years, the Boom Clay hydraulic conductivity K has been determined in several ways and at several scales (Yu *et al*., 2011, 2013).

Most of the K-values were obtained from **laboratory experiments** on core samples including both percolation experiments used in the framework of migration studies (samples with sizes of 36 cm^3 and 82 cm^3) and hydraulic conductivity tests using permeameter (57 cm^3)/isostatic (1.5 dm^3)/triaxial apparatus (46 cm^3 and 94 cm^3). Imposed hydraulic gradients in percolation and permeameter tests normally are much larger than the natural hydraulic gradient. However, for constrained Boom Clay samples and within the studied range of gradients, the influence of the gradient on the hydraulic conductivity is negligible and Darcy's Law can be considered valid (Volckaert *et al*., 1995; Marivoet *et al*., 2009).

Small-scale *in situ* tests using piezometers were performed at the HADES URF through either single point tests assuming isotropy of flow (measurement volume equals several thousand cm^3) or interference tests with multi-piezometers, with which oriented (K_h and K_v) values of hydraulic conductivity can be derived.

A **large-scale *in situ* test** was carried out at the HADES URF by measuring the water infiltration rate into an experimental gallery during 3 years, considering a measurement volume of at least several hundred m^3.

<u>Boom Clay hydraulic conductivity at the Mol site</u>
A large fraction of the hydraulic conductivity data of the Boom Clay at the Mol site is associated with the Mol-1 borehole (Wemaere *et al*., 2002), providing a detailed hydraulic conductivity profile of the entire Boom Clay at a vertical spatial resolution of 1-2 m. Both K_h and K_v were measured by means of permeameter and percolation tests (Wemaere *et al*., 2002, 2008). The main

stratigraphic sub-units for the Mol-1 borehole together with their respective K_h and K_v values are listed in Table 4.

Additionally, the HADES URF, where *in situ* tests were performed and numerous Boom Clay samples were taken for laboratory K determination, provides supplementary information on K-values for the central part of the Boom Formation. Most in situ tests were carried out in the Putte Member, while only one (R13U) in the Boeretang Member and another (MORPHEUS) in the Terhagen Member.

Table 4: Vertical (K_v) and horizontal (K_h) hydraulic conductivity in Boom Clay, measured on samples from the Mol-1 borehole (Yu *et al.*, 2013 - after Wemaere *et al.*, 2002)

Member	Vertical hydraulic conductivity			Horizontal hydraulic conductivity		
	N	K_v (m/s)	s	N	K_h (m/s)	s
Boeretang	16	2.8×10^{-12}	0.2	3	5.0×10^{-12}	0.1
Putte	29	2.4×10^{-12}	0.2	12	4.8×10^{-12}	0.1
Terhagen	9	2.0×10^{-12}	0.1		6.2×10^{-12}	0.2
Belsele-Waas	10	1.6×10^{-11}	1.0	5	5.7×10^{-11}	1.2
Boom Clay unit	64	2.8×10^{-12}		20	1.3×10^{-11}	

K values for Boom Clay members are geometric means: $K_{geom}=\sqrt[n]{K_1 \cdot K_2 \cdots K_n}$ $\sqrt{K1 \cdot K2 \cdots Kn}$, Boom Formation *K* value is the harmonic mean for K_v and arithmetic mean for K_h weighted by the thickness of each member; s is the standard deviation of log(*K*).

Figure 10 provides a vertical profile of the K-values for the entire section of the Boom Formation at the Mol site with indication of the main stratigraphic member and the test type. The clay, silt and sand content profile measured from the Mol-1 borehole is also illustrated. Geometric mean vertical (K_v) and horizontal (K_h) hydraulic conductivities derived from laboratory tests and equivalent hydraulic conductivities (K) obtained from *in situ* tests are illustrated respectively by the dashed, dash-dotted and solid lines for each member. For Putte and Terhagen Members, the equivalent K from *in situ* tests lies in between K_v and K_h derived from the laboratory tests. This is due to the working principle of the single point piezometer test assuming isotropic flow.

The typically banded nature of the Boom Clay, resulting in an alternation of more silty and more clayey beds, is not represented in the hydraulic conductivity values (Figure 10). Vertical hydraulic conductivity variations across the clay formation can however be distinguished. According to Figure 10 and Table 4, the overall highest mean K-values and highest heterogeneity are measured for the Belsele-Waas Member (geometric mean $K_v = 1.6\times10^{-11}$ m/s, $K_h = 5.7\times10^{-11}$ m/s; standard deviation s of the log transformed K values is 1.0 and 1.2 for respectively K_v and K_h) and are attributed to its high sand content of 22 % on average. The Putte and Terhagen Members, which represent the central part of the Boom Formation, show the lowest overall mean values of hydraulic conductivity (geometric mean $K_v = 2.4\times10^{-12}$ m/s and $K_h = 4.8\times10^{-12}$ m/s for Putte and geometric mean $K_v = 2.0\times10^{-12}$ m/s and $K_h = 6.2\times10^{-12}$ m/s for Terhagen) and display the lowest heterogeneity with depth (s is smaller than 0.2), except for the sandy 'double band' in the lower Putte Member. The very silty bed of the Boeretang Member yields similar or slightly higher K values than the Putte and Terhagen Members (geometric mean $K_v = 2.8\times10^{-12}$ m/s and $K_h = 5.0\times10^{-12}$ m/s), but with some more variation according to depth.

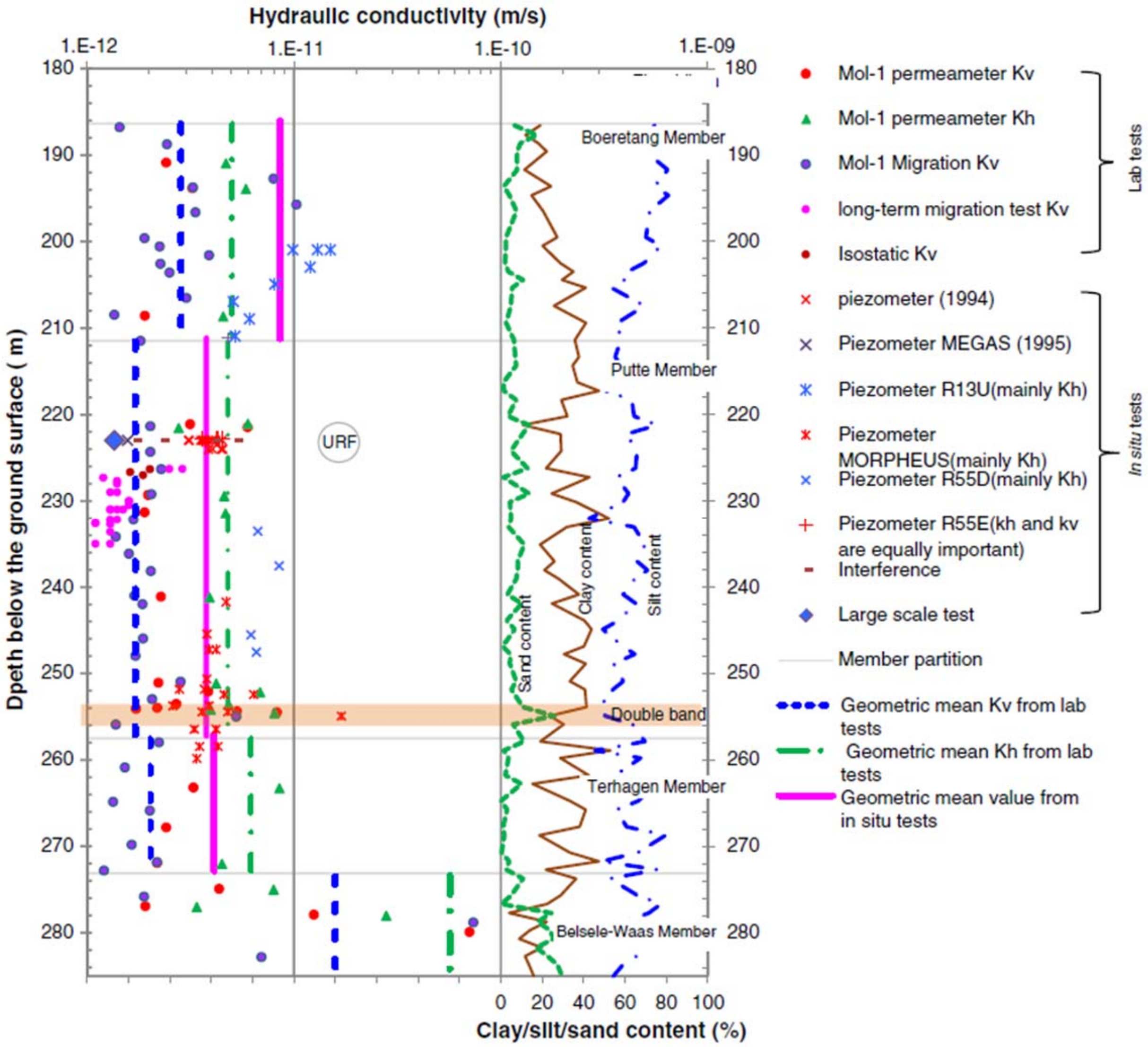

Figure 10. Hydraulic conductivity profile of Boom Clay at the Mol site based on lab tests and *in situ* tests at the HADES URF (Yu *et al*., 2013).

The summary of hydraulic conductivities measured from various techniques for the Putte and Terhagen Members in Figure 11 reveals a very consistent estimate of the hydraulic conductivity considering the 95 % confidence intervals. According to Figure 11, *in situ* measurements of the hydraulic conductivity of the Boom Clay made on a few decimeters-long filters and on a meters-long gallery at the HADES URF yield values that are very similar (geometric mean $K = 3.5\times10^{-12}$ m/s for piezometer tests and 1.4×10^{-12} m/s for large-scale *in situ* test) to the values measured in the laboratory on samples with a thickness of a few centimeters (geometric mean $K_v = 1.9\times10^{-12}$ and $K_h = 4.3\times10^{-12}$ m/s). Consequently, parameter values measured on a centimeter scale can also be applied when the scale is upscaled to meters, for so far as the considered clay volume can be considered as homogeneous for that parameter (Marivoet *et al*., 2009). Moreover, the scale dependency of the hydraulic conductivity in the Boom Clay was also studied by Huysmans (2006), who compared results of groundwater flow and transport models using heterogeneous hydraulic conductivity fields, and a single value of hydraulic conductivity (which is equivalent to a large scale K). The resulting fluxes differed only slightly, which indicates a small effect of scale on the hydraulic conductivity value.

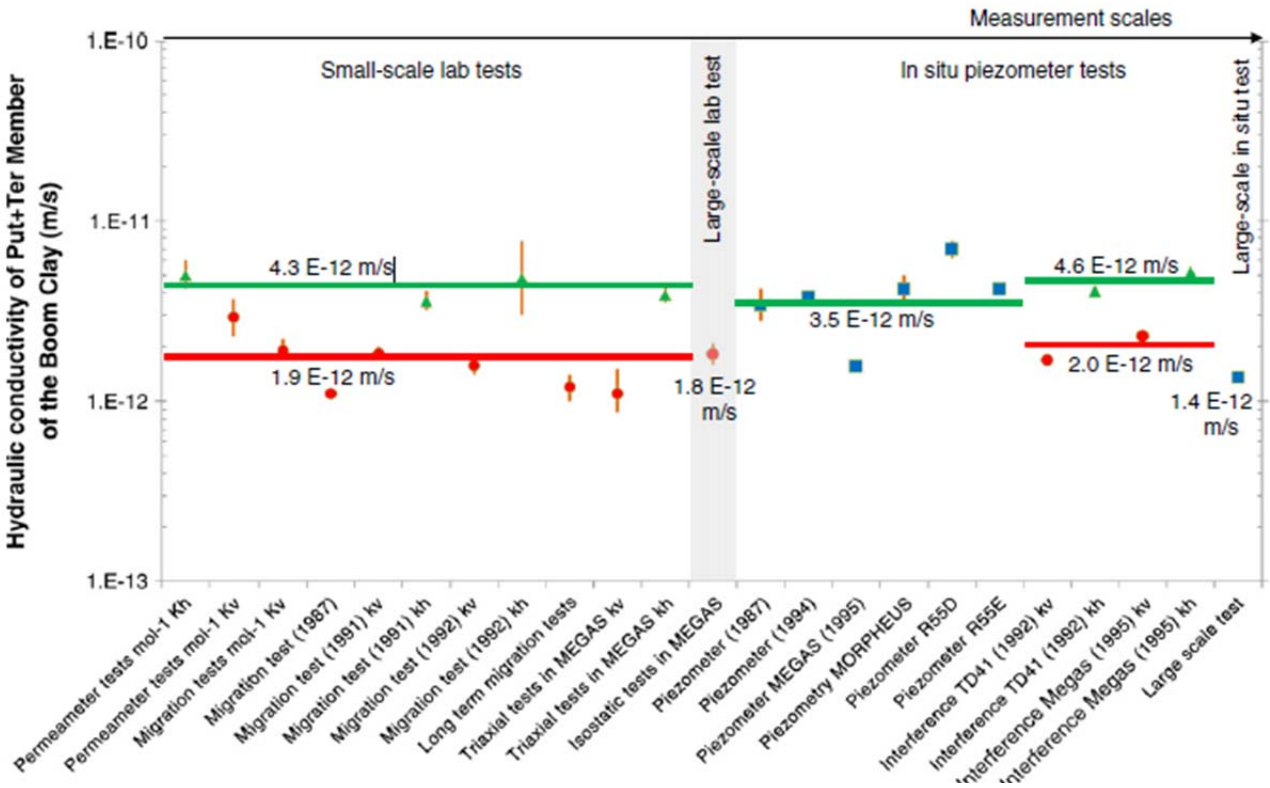

Figure 11. Overview of hydraulic conductivity values (m/s) for Putte and Terhagen Members at the Mol site. Vertical bars represent the 95 % confidence interval (Yu *et al.*, 2013).

Although the Mol-1 borehole revealed hydraulic conductivity data on the entire Boom Clay profile, most data obtained from *in situ* experiments from the HADES URF only give information on the Putte and Terhagen Members. Taking into account all the measured data in the Putte and Terhagen Members at the Mol site, the geometric mean of the vertical and horizontal hydraulic conductivities are 1.7×10^{-12} m/s and 4.4×10^{-12} m/s respectively, with an anisotropic ratio of about 2.5 (Yu *et al.*, 2011).

CONCLUSION: the results of the various lab-experiments and *in situ* measurements at different scales (summarized in Yu *et al.*, 2011 and Yu *et al.*, 2013) yielded consistent hydraulic conductivity values and indicate that Boom Clay at the Mol site has a very low hydraulic conductivity in general, in the order of 10^{-12} m/s. The Putte and Terhagen Members, representing the central part of the Boom Formation, show the lowest overall mean *K*-values, while the more sandy Belsele-Waas Member (bottom of Boom Clay) and to a lesser extent also the silty Boeretang Member (top of Boom Clay) display higher *K*-values.

<u>Regional variability in Boom Clay hydraulic conductivity</u>

The regional variability of the Boom Clay hydraulic conductivity was studied by regional borehole investigations in the Campine area, including the Doel-2b, Zoersel, Mol-1, Weelde-1 and Essen-1 boreholes (Wemaere *et al.*, 2002, 2004a, 2005, 2008; Labat *et al.*, 2008a). Figure 12 illustrates the regional extent of the Boom Clay, its thickness, its depth below surface, and the locations of the five investigation boreholes. For each borehole, the vertical and horizontal hydraulic conductivity were measured experimentally using permeameter and percolation experiments on clay cores which were sampled over the entire Boom Clay profile.

Table 5 summarizes the Boom Clay hydraulic conductivity data for the five boreholes. The spatial variability in hydraulic conductivity according to the stratigraphic sub-units is displayed in Figure 13.

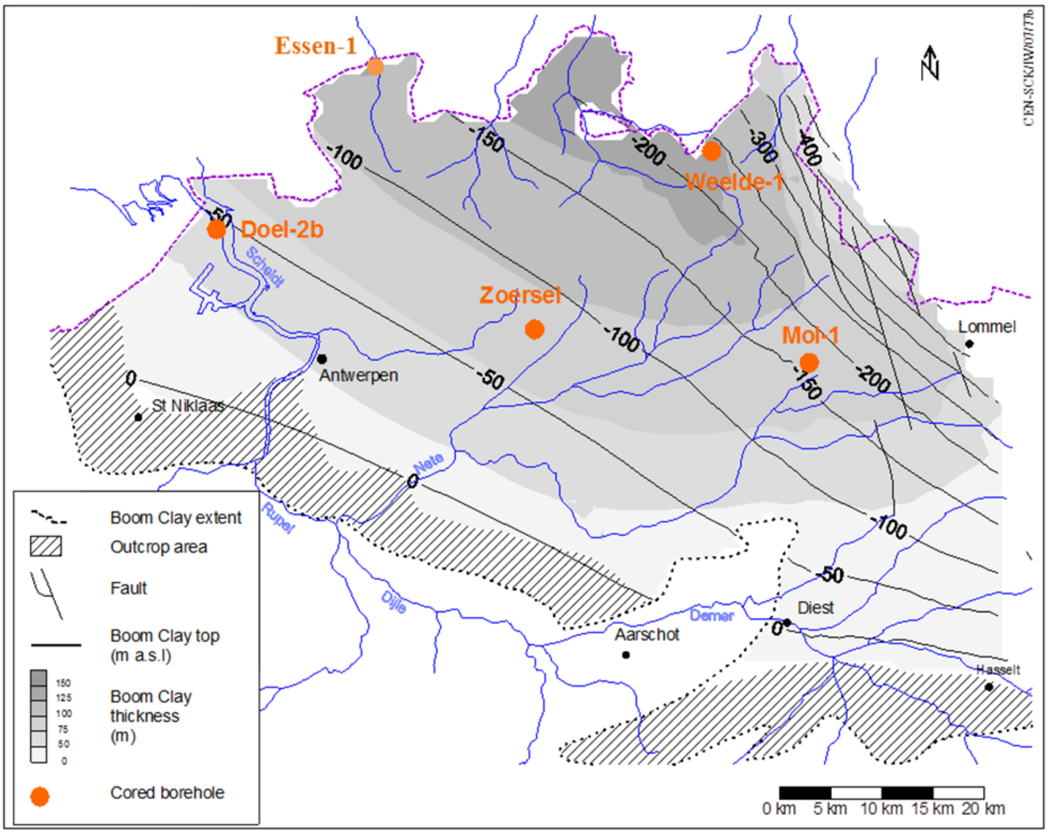

Figure 12: Geographic extent of the Boom Clay in NE-Belgium with indication of depth and thickness. (Wemaere *et al*., 2008; Yu *et al*., 2011).

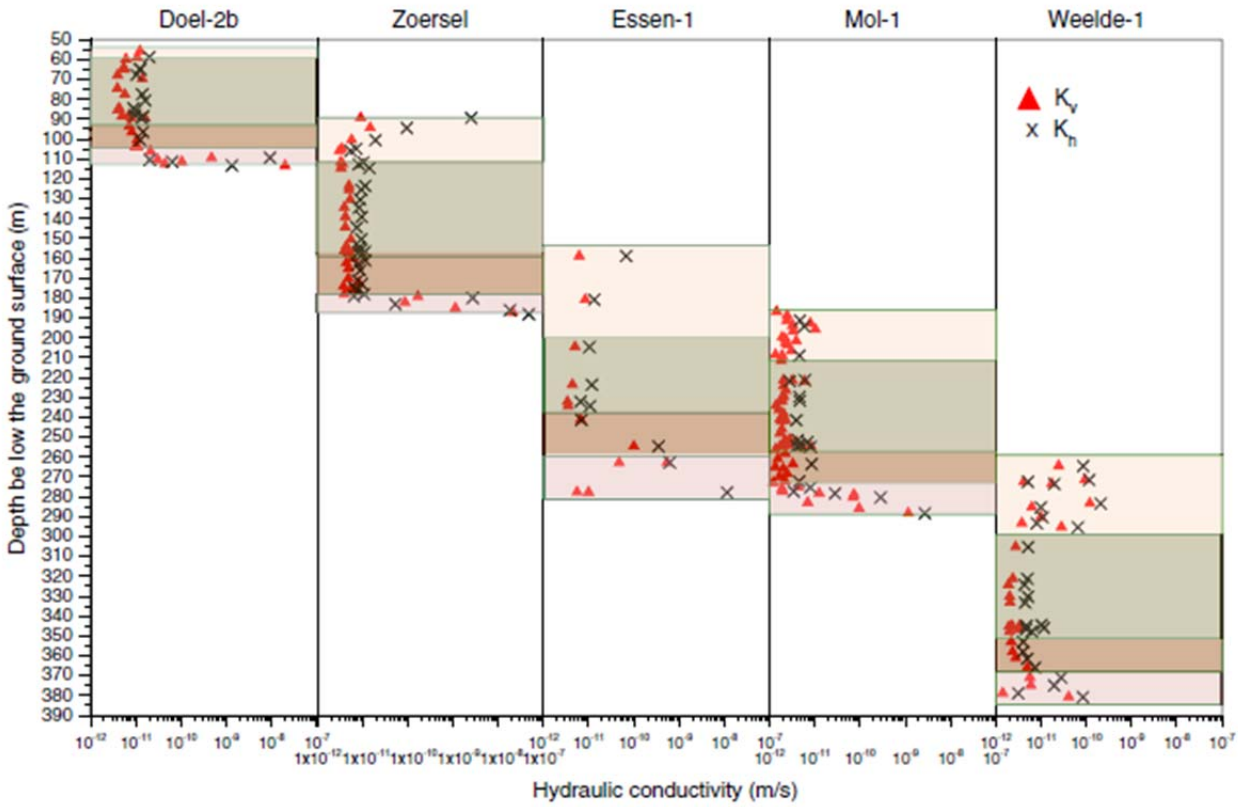

Figure 13. Spatial variability of hydraulic conductivity in five boreholes. Sub-units for all boreholes are identical (from top to bottom): Boeretang Member, Putte Member, Terhagen Member, and Belsele-Waas Member (Yu *et al.*, 2013)

A typical K profile of the Boom Clay observed in all boreholes exhibits a less permeable and relatively more homogeneous central Putte and Terhagen Member, and a more permeable and heterogeneous overlying Boeretang Member and underlying Belsele-Waas Member.

With respect to the vertical hydraulic conductivity, the Essen-1 and Doel-2b boreholes have a pronounced higher global mean value for the entire Boom Clay than the other boreholes (Table 5) ($K_v = 8.5\times10^{-12}$ m/s and $K_v = 8.0\times10^{-12}$ m/s respectively). The Mol-1 borehole appears to be the least permeable one ($K_v = 2.8\times10^{-12}$ m/s). An increase in hydraulic conductivity is observed from east towards the west, *i.e.* increasing from Mol → Weelde → Zoersel → Doel → Essen. A similar trend is observed for K_h, with Essen-1 having the highest overall K_h (4.7×10^{-10} m/s).

Generally, the vertical hydraulic conductivities of the Putte and Terhagen Members are in the order of 10^{-12} m/s in all boreholes (Table 5). The variation with depth is also the smallest for the Putte and Terhagen Members with the standard deviation of the log transformed K values between 0.1 and 0.2, except for the Doel-2b and Essen-1 boreholes where it reaches 0.8 and 0.5, respectively. The Boeretang Member is slightly more permeable than the Putte and Terhagen Members in the Zoersel, Essen-1 and Mol-1 boreholes (less than a factor 2, except for the K_h in Zoersel), and somewhat more permeable in the Weelde-1 and Doel-2b boreholes. The Belsele-Waas Member is only slightly more permeable than the Putte and Terhagen Members in the Weelde-1 borehole (a factor 2.6 for K_v and 3.6 for K_h), but much more in other boreholes, especially in the Zoersel borehole (a factor of 160 for K_v and 370 for K_h). The Belsele-Waas Member displays in the five boreholes the highest values of the standard deviation of the log transformed K values, i.e. from 0.4 to 1.2. The Weelde-1 borehole exhibits the lowest variations of

K in the Belsele-Waas Member, while Mol-1 displays the highest variation (s = 1.0 for K_v and s = 1.2 for K_h).

Most of the analyses yield an anisotropy ratio at the sample scale (57 cm^3 in permeameter test) of about 2 (Wemaere *et al*., 2002, 2004a-b, 2005, Aertsens *et al*. 2005, Labat *et al*., 2008a-b). However, calculating the harmonic means at the scale of the formation thickness (about 100 m) leads to an increased global anisotropy ratio at the formation scale of about 3-7 in the case of the Mol-1, Doel-2b and Weelde-1 boreholes and nearly 60 for the Zoersel and Essen-1 boreholes. It is the contrasting nature of the individual Boom Clay members, in particular the Belsele-Waas Member that is mainly responsible for the increased calculated anisotropy at the formation scale (Wemaere *et al*., 2008).

The statistical analysis of the five boreholes (Yu *et al*., 2013) implies that regional variation in K_v of the Boom Clay can be attributed in part to the porosity variation of the Boom Clay, which is related to the burial depth of the clay and which is increasing from the southwest towards the northeast. A second variable which explains part of the variation in K_v is the grain-size parameter *d*40, which is defined as the grain-size (µm) for which 40% of the particles are finer. There are further indications that decreasing porosity with depth explains part of the *K* variation across the investigated area. However, part of the variation in K_v remains unexplained. A similar conclusion was put forward by Jeannée et al. (2013), who did a geostatistical analysis of the vertical hydraulic conductivity of the Boom Clay: their analysis led to the conclusion that regional anomalies in *Kv* exist, which have not been fully explained so far. Effects of possible other factors on *K* variability, such as mineralogy, carbonate content, overconsolidation,… were not investigated in these studies due to lack of information.

CONCLUSION: the results finally demonstrate that the hydraulic conductivity of the Boom Clay, especially in the Putte and Terhagen Members, remains very consistent even for the relatively large geographical area of NE-Belgium. However, unexplained regional variations still exist today.

Table 5: Overview of the K values at the five regional cored boreholes (Yu *et al*., 2011, 2013).

Unit	Doel-2b			Zoersel			Essen-1			Mol-1			Weelde-1		
	n	*K*	s	n	*K*	s	n	*K*	s	n	*K*	s	n	*K*	s
	K_v (m/s)														
Boeretang	2	1.2×10^{-11}	0.03	6	5.5×10^{-12}	0.3	2	7.2×10^{-12}	0.1	16	2.8×10^{-12}	0.2	9	1.7×10^{-11}	0.5
Putte & Terhagen	18	6.6×10^{-12}	0.8	24	4.8×10^{-12}	0.1	6	7.5×10^{-12}	0.5	38	2.3×10^{-12}	0.2	15	2.6×10^{-12}	0.2
Belsele-Waas	6	1.8×10^{-10}	1.0	4	7.7×10^{-10}	0.9	4	3.5×10^{-11}	0.8	10	1.6×10^{-11}	1.0	4	6.7×10^{-12}	0.4
Entire Boom Clay	26	8.0×10^{-12}		34	5.5×10^{-12}		12	8.5×10^{-12}		64	2.8×10^{-12}		28	4.0×10^{-12}	
	K_h (m/s)														
Boeretang	1	2.0×10^{-11}	-	6	3.5×10^{-11}	1.0	2	3.0×10^{-11}	0.5	3	5.0×10^{-12}	0.1	9	2.9×10^{-11}	0.6
Putte & Terhagen	12	1.2×10^{-11}	0.1	23	9.0×10^{-12}	0.1	6	1.7×10^{-11}	0.7	12	5.0×10^{-12}	0.1	15	5.5×10^{-12}	0.2
Belsele-Waas	4	3.6×10^{-10}	1.1	4	3.4×10^{-9}	1.1	2	2.7×10^{-9}	0.9	5	5.7×10^{-11}	1.2	4	2.0×10^{-11}	0.7
Entire Boom Clay	17	5.7×10^{-11}		33	3.2×10^{-10}		10	4.7×10^{-10}		20	1.3×10^{-11}		28	1.5×10^{-11}	

n: number of analyses; s: standard deviation of Log(*K*)

K_v & K_H: sub-unit values are geometric means, Boom unit K value is the harmonic mean for K_v and arithmetic mean for K_h weighted by the thickness of each sub-unit

s: standard deviation of Log(*K*)

3.3. Hydrogeological context: Hydraulic gradient, Darcy velocity and Péclet number

The hydraulic gradient (i) is a vector gradient between two or more hydraulic head measurements over the length of a flow path:

$$i = \frac{dh}{l} = \frac{h_1 - h_2}{l} \quad \textbf{Equation 8}$$

Where i is the hydraulic gradient [-], dh is the difference between two hydraulic heads (h_1 and h_2) [m] and l is the length between two points at which the difference in the hydraulic heads was measured [m]. It is important to note that the gradient is measured along a flow path, e.g. along the line of the largest possible slope of the groundwater flow.

In case of the Boom Clay, the flow path is assumed to be nearly vertical. This assumption is based on the Boom Clay low hydraulic conductivity and its regional continuity. Given the flow follows the path of the lowest resistance, the flow path in the Boom Clay (and any regional aquitard) is perpendicular to the bedding, since the hydraulic resistance in this direction is the smallest due to the smallest distance to overcome.

Using the assumption of the nearly vertical flow path across the Boom Clay, the Boom Clay gradient is calculated as the difference in the groundwater levels in the aquifers above and below the Boom Clay, divided by its thickness. The most suitable measurements for the gradient estimation are coming from the multi-piezometers which monitor the groundwater level above and below the Boom Clay.

Sources of information are groundwater level measurements in the aquifers above and below the host rock, summarized in the report on 30 years of regional groundwater monitoring (Labat, 2011), supplemented by piezometric measurements of the VMM (DOV, 2011). Furthermore, in the frame of regional groundwater modelling, a specific transient model was developed that investigates the effects of groundwater overexploitation in the aquifers below the Boom Clay (Vandersteen *et al.*, 2012). This model was used to calculate the vertical velocity over the Boom aquitard in NE-Belgium as well as the Péclet numbers in the Boom Clay on a regional scale.

3.3.1. Hydraulic gradient at the Mol site

At the Mol site, the hydraulic gradient is estimated using the piezometric measurements on site 15 (Labat, 2011). As seen in Figure 14B, the estimated gradient increases in time from about 0.015 in the beginning of the eighties to about 0.043 in 2012. This increase is caused by the decreasing groundwater head in the Oligocene aquifer (Figure 14A) caused by the overexploitation of the Oligocene and Ledo-Paniselian-Brusselian aquifer systems. The hydraulic gradient over the Boom Clay is also varying seasonally, whereby the seasonal variation in the groundwater levels in the aquifers above the Boom Clay influences the estimated gradient. However, the seasonal influence is significantly smaller (magnitude about 0.01) than the influence of the pumping. The hydraulic gradient over the Boom Clay at the Mol site is low and vertically downward oriented.

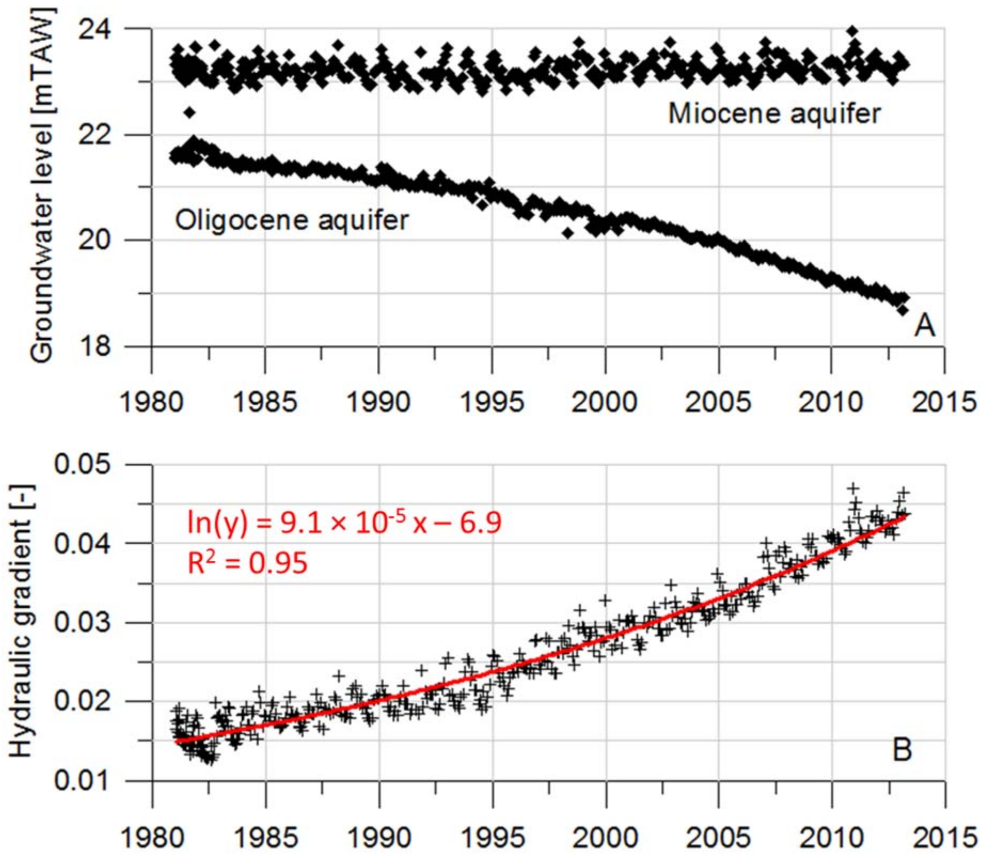

Figure 14: Groundwater level measurements (A) in the Miocene aquifer (above the Boom Clay) and the Oligocene aquifer (below the Boom Clay) and the estimated hydraulic gradient (B) at piezometer site 15.

3.3.2. Regional variability in hydraulic gradient and vertical Darcy velocity

At a regional scale, the hydraulic gradient is not constant. Figure 15 shows the average hydraulic gradient calculated from the 30 years of piezometric measurements (Labat, 2011) and from the VMM (DOV, 2011). The average, minimum and maximum values of the hydraulic gradient over the Boom aquitard per piezometer time series are given in Table 6. The hydraulic gradient vectors are pointing both upward and downward and the average values per piezometer range from -0.034 to 0.75 (Table 6). In most cases, there is less than a factor 2 difference between the minimum and maximum gradient values at the same piezometer. However, in some cases, the differences are higher (up to a factor 12), but these are situated at locations with very low gradients.

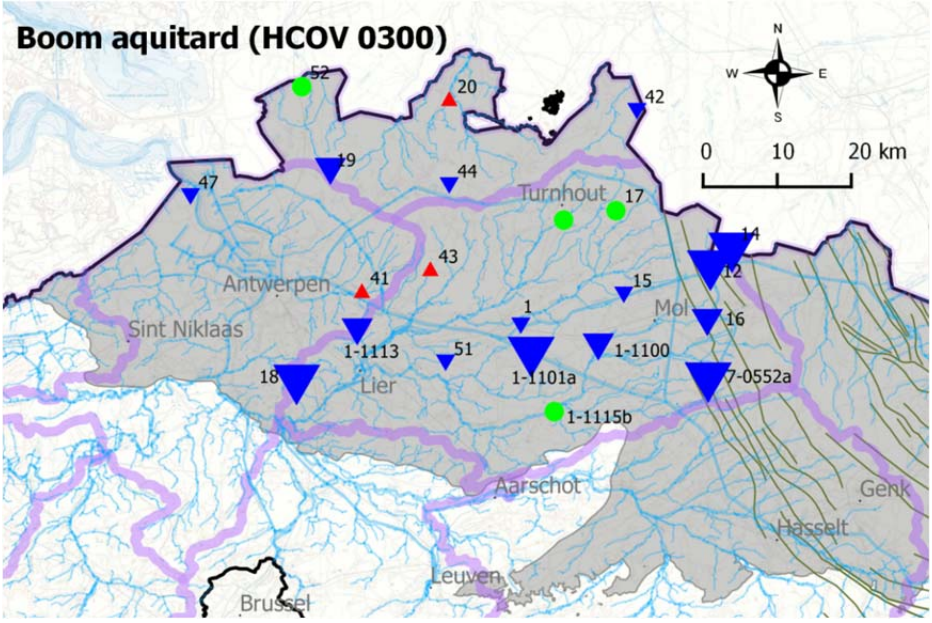

Figure 15: Estimated hydraulic gradient over the Boom Clay (after Vandersteen *et al*., in prep.).

Table 6. Average, minimum and maximum gradient over the Boom aquitard per groundwater head time series. (Vandersteen *et al*., in prep.).

name	x	y	Average of gradient	Min of gradient	Max of gradient	thickness Boom aqt. (m)
15	198409	211736	0.026094	0.014696	0.043366	101
16	208980	208200	0.096659	0.077679	0.103266	99
17	197390	222680	0.002273	0.00082	0.010274	121
18	156020	200694	0.751147	0.627417	0.874977	40
19	160141	227764	0.072779	0.065736	0.078489	111
20	175740	236842	-0.03364	-0.02684	-0.03845	141
41	164455	212040	-0.03098	-0.01536	-0.05329	78
42	200069	235536	0.015348	0.008021	0.028103	128
43	173322	214845	-0.03385	-0.03083	-0.03567	98
44	175780	225883	0.046636	0.039166	0.050797	112
45	190552	221424	-0.00694	-0.0035	-0.00846	123
47	142221	224446	0.022123	0.009158	0.037568	74
51	175303	202909	0.032593	0.029344	0.038042	80
52	156662	238672	0.003999	0.001165	0.007292	128
1-1100	194861	205033	0.057481	0.051924	0.064752	101
1-1101a	186409	204300	0.153433	0.151833	0.154583	90
1-1113	163620	206993	0.086705	0.079695	0.104078	77
1-1115b	189388	196607	-0.00133	-0.00957	0.014811	53
7-0552a	209350	200985	0.225975	0.151538	0.265632	57
1	185001	207740	0.02985	0.011412	0.049592	98
12	209640	215490	0.148695	0.087967	0.16385	100
14	212425	217790	0.143556	0.132549	0.157333	100

The variability of the average gradients is above all caused by the differences in spatial groundwater level distribution between the shallow and deep aquifer systems. In the shallow aquifer system, the groundwater circulation is governed by infiltration and drainage by the rivers. Higher gradients pointing downwards occur then at places where the upper aquifer heads are elevated, typically at the catchment boundaries or the fault system of the Roer Valley Graben. Inversely, upward gradients are found where the heads in the upper aquifer are relatively low – close to the rivers or towards the west – close to the Scheldt estuary. In the deep aquifer system, if not perturbed by pumping, the groundwater level distribution would be rather monotonous due to the lack of internal sources and sinks. The excessive pumping in the aquifers below the Boom Clay caused large head drops close to the pumping wells. This was observed in areas where these aquifers occur at shallow or moderate depth, which leads to high hydraulic gradients over the Boom Clay. Currently, the pumping influence does not reach the northernmost piezometers.

Under assumed natural conditions, low upward gradients would form along the principal rivers, resulting from differences between the topographic height of the Oligocene recharge area and the river water level. In case of a downward gradient, a moderate magnitude can be reached along the catchment boundaries, where the heads in the aquifers above the Boom Clay are relatively elevated. The overexploitation of the aquifers below the Boom Clay artificially increases the difference in the groundwater levels below the Boom Clay, causing or increasing the downward gradient.

The Boom Clay thickness influences the gradient value only marginally, since the Boom Clay thickness varies from approx. 40 meters at the outcrop (site 18) to approx. 145 meters at the northern Belgian border (site 20). Such difference attributes to about a factor 4 difference in the gradient value.

Figure 16 shows the vertical Darcy velocity through the Boom Clay as calculated by the Deep Aquifer Pumping model (DAP – Vandersteen *et al.*, 2012). Under natural conditions, without pumping in the Oligocene and the Ledo-Paniselian-Brusselian aquifers, the areas with downward flow are situated close to the outcrops in the south (where the thickness of the Boom Clay is low) and at the more elevated areas, i.e. the Campine plateau in the east and the water divide between the Meuse and Scheldt catchment at the Campine cuesta to the north. The topographically lower areas, i.e. central part of the Nete catchment or Scheldt estuary close to Antwerp, are generally featuring upward flow, meaning that the water seeps up to the Miocene aquifer through the Boom Clay. The velocities are generally very small. Under the presence of pumping, the downward flow area increases substantially. More is recharged close to the outcrops, where the pumping wells are located in the Oligocene, featuring also higher vertical velocities here. Further away from the outcrops, more to the north, the velocities remain very small (< 1 mm/yr).

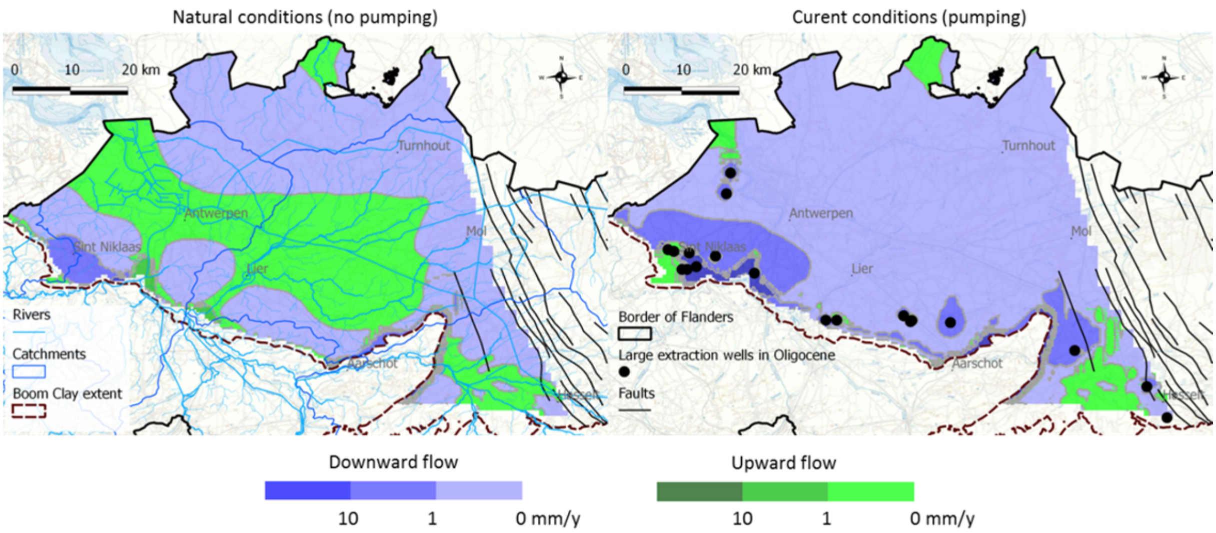

Figure 16. Vertical Darcy velocity through the Boom Clay simulated by the DAP model (Vandersteen *et al.*, 2012) under assumed natural conditions (left) and under current conditions (right) involving pumping in the Oligocene aquifer. (Vandersteen *et al.*, in prep.).

3.3.3. Derivation of Péclet numbers on the regional scale

This section gives an indicative calculation of the Péclet numbers in the Boom Clay on the regional scale. An appropriate Péclet number definition for low-permeability media is applied to the Boom Clay to give an indication about the governing transport mechanisms. The applied Péclet number definition is (SAFIR 2, 2001):

$$\boldsymbol{Pe} = \frac{\boldsymbol{v_D x}}{\boldsymbol{\eta R D_{app}}} \qquad \textbf{Equation 9}$$

Where v_D is the Darcy velocity [m/s], x is a characteristic length [m], η is the diffusion accessible porosity [-], R is the retardation factor [-] and D_{app} is the apparent diffusion coefficient [m^2/s].

At a spatial scale defined by the reference length L, advection is dominant over molecular diffusion if $Pe >> 1$, and molecular diffusion is dominant if $Pe << 1$ (Soler, 2001).
The (vertical) Darcy velocity was derived in the previous section (Figure 16). On a regional scale, the product of R with the diffusion accessible porosity for HTO varies between 0.37 and 0.42 (Table 2), the measured apparent diffusion coefficient of HTO varies between 1.3×10^{-10} m^2/s and 2.8×10^{-10} m^2/s (Aertsens *et al.*, 2010) and the distance to the source varies from 0 to half the thickness of the Boom Clay. We calculated the Péclet numbers from the DAP-model (Vandersteen *et al.*, 2012) on a regional scale using the most adverse parameters (x = half the thickness of the Boom Clay, $D_e = 1.3\times10^{-10}$ m^2/s, $\eta = 0.37$) (Figure 17) in the case without pumping (natural conditions) and for the year 2010.
From Figure 17, it can be seen that the Péclet numbers in the Boom Clay are quite variable on the regional scale, both under natural conditions and in the 2010 case (including current pumping in the Oligocene aquifer). Values above 1 are reached only close to the outcrop of the Boom Clay, where the pumpings are situated. At the Mol site, the Péclet number calculated using the most adverse parameters is less than 1 in both cases.

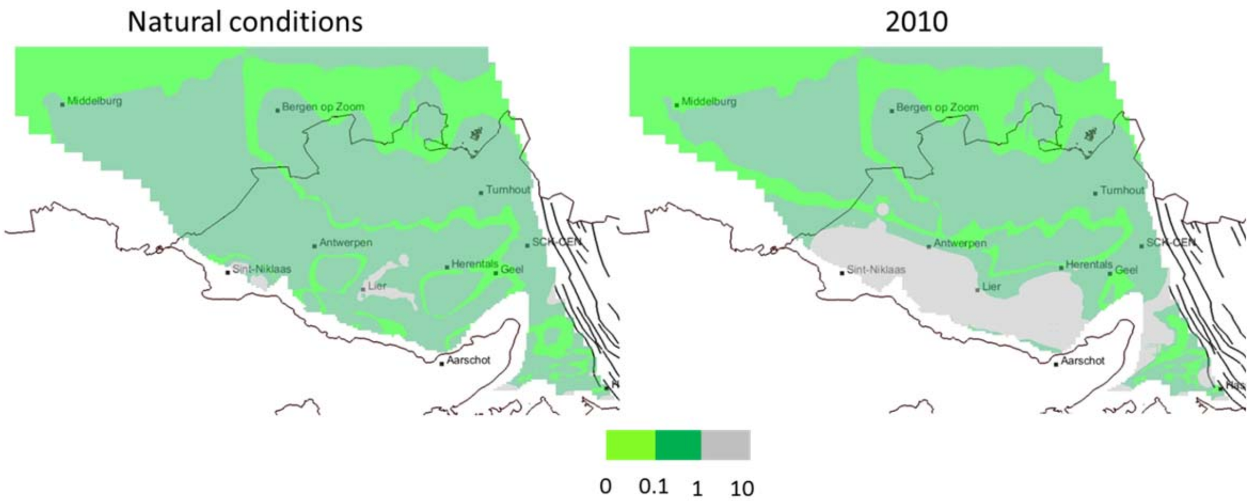

Figure 17. Regional Péclet number values using the most adverse input parameters under natural conditions (without pumping) and in the 2010 situation (including pumping in the Oligocene aquifer).

CONCLUSION: The hydraulic gradient over the Boom Clay at the Mol site is low and vertically downward oriented. On the regional scale, both upward and downward gradients exist, which can be considerably influenced by pumping. Very small vertical velocities were calculated in areas without groundwater extractions in the Oligocene aquifer. The regional Péclet numbers, calculated using the most adverse parameters,

indicate a large variability over the study area. Close to the outcrops higher values (> 1) can be reached.

3.4. Preferential flow or conducting features

Boom Clay contains two features which might favour preferential flow: fractures, and carbonate-rich layers containing septarian carbonate concretions. In this section, these possible conducting features are discussed.

3.4.1. Fractures

Natural discontinuities in the Boom Clay have been observed in the outcrop area near Antwerp. Subvertical joints are a common feature for the Boom Clay occurring near the surface (max. depth 40-50 m, Mertens et al., 2003), whereas a normal fault zone has been observed in only one clay-pit in Kruibeke (Vandenberghe et al., in prep.).

At depth (Mol site), natural fractures through Boom Clay have not been observed so far. However, excavation-induced fractures do occur around the HADES galleries. Fractures in the Boom Clay were studied by Bernier *et al*. (2004, 2007) and Bastiaens *et al*. (2007) (SELFRAC project), Chen *et al*. (2010) and Yu *et al*. (2010) (TIMODAZ project) and Huysmans (2006).

Within the SELFRAC project, different experiments demonstrated that the swelling clay minerals and the visco-elasto-plastic behaviour of the Boom Clay seal fissures under saturated conditions and normal geomechanical stress (Bastiaens *et al*., 2007; Bernier *et al*., 2004; Bernier *et al*., 2007). Note the difference between sealing and healing of fractures. Sealing is the reduction of fracture permeability by any hydromechanical, hydrochemical, or hydrobiochemical processes. Healing, on the contrary, is sealing with loss of memory of the pre-healing state. Thus, for example, a healed fracture will not be a preferred site for new fracturing just because of its history. Sealing (and healing) is in general the result of several mechanisms. The main mechanisms for sealing (and healing) in clays are swelling, consolidation and creep.

In situ observations at the HADES URF have led to a good understanding and characterization of excavation induced fractures around shafts and galleries. Around the connecting gallery, fractures have a radial extent of 1 m into the host rock and they originated about 6 m ahead of the excavation face. Fractures seal but can be reactivated. At present, no unsealed fracture network exists beyond (at most) some decimetres into the host rock (Bastiaens *et al*., 2007).

Steady state, *in situ*, constant head tests showed an increase of hydraulic conductivity up to 6-8 m around the connecting gallery (Figure 18). The values outside this influenced zone are about 6×10^{-12} m/s and 4×10^{-12} m/s, measured on a vertical and a horizontal piezometer respectively. At the measuring points closest to the gallery, K is one order of magnitude larger than the undisturbed value and a decreasing trend with time was observed. Furthermore, the authors conclude that effective stress variation alone can account for the variation of hydraulic conductivity measured around the connecting gallery and that the influence of fractures is not important.

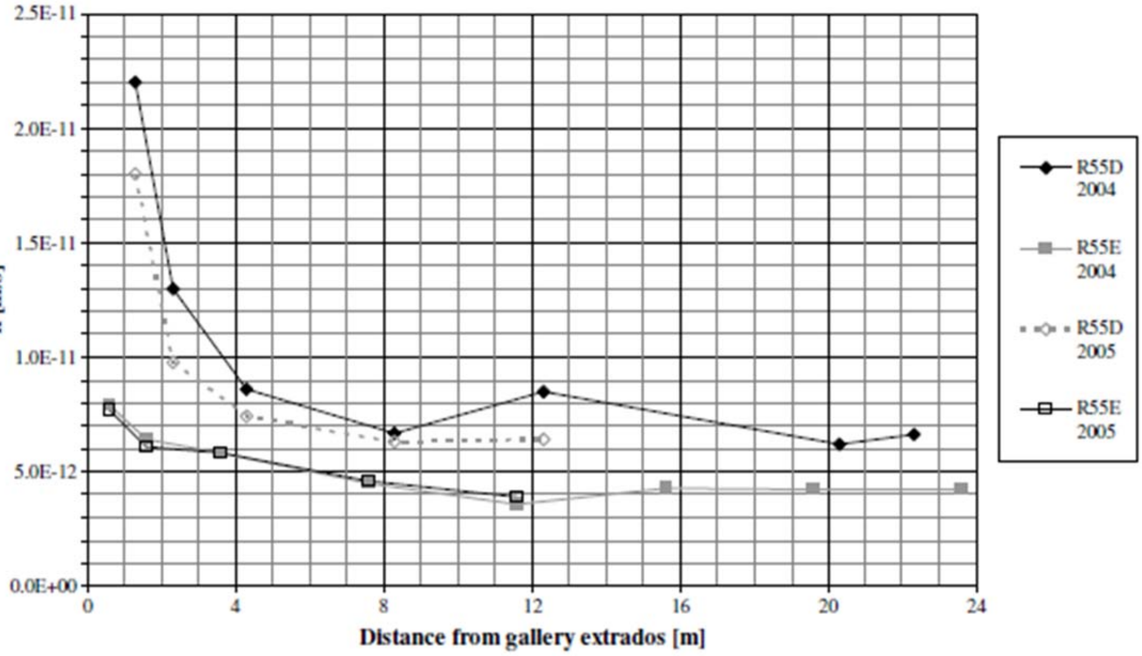

Figure 18. Results of steady state, constant head measurements of the hydraulic conductivity around the connecting gallery performed on a horizontal (R55E) and a vertical (R55D) piezometer in 2004 and 2005 (Bastiaens *et al.*, 2007).

Sealing effects in Boom Clay are very fast as shown, for instance, by µCT images of an artificially fractured clay sample (30.3 mm high, diameter 38 mm). The images were taken before and after hydraulic conductivity measurement on the sample and indicate closure of the fracture, only due to saturation of the sample. The µCT images are shown in Figure 19 (a) (before saturation) and Figure 19 (b) (after 4.5 h of hydraulic conductivity measurement). Sealing was confirmed by the results of the hydraulic conductivity measurements on the sample, which were of the same order of magnitude as the undisturbed value, being 10^{-12} m/s.

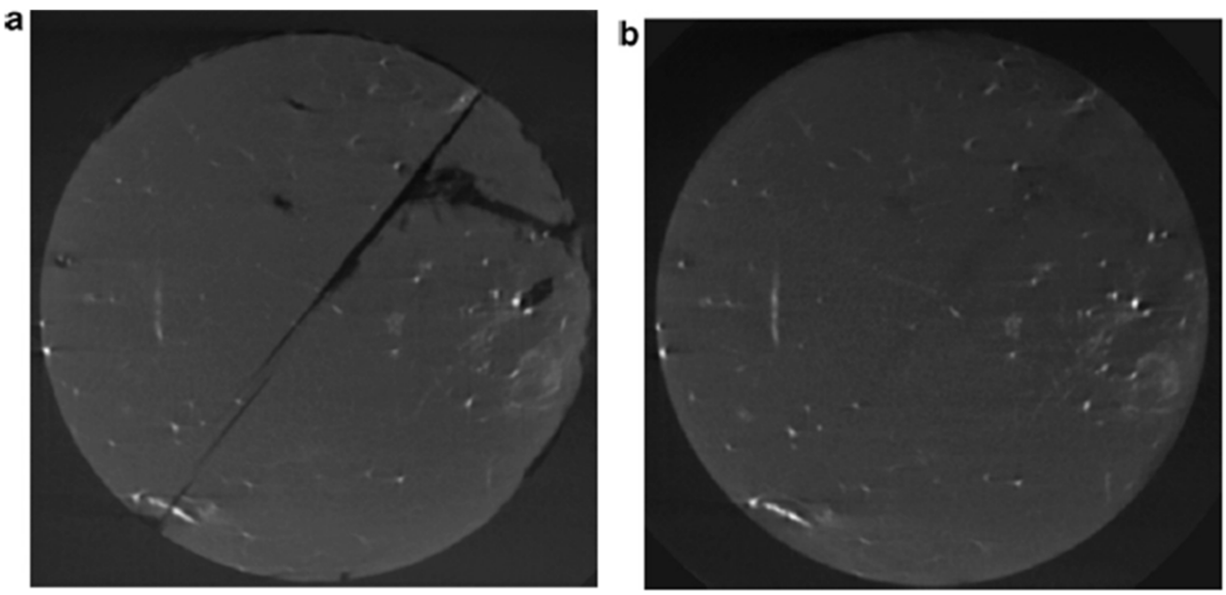

Figure 19. µCT images of an artificially fractured clay sample (30.3 mm high, diameter 38 mm). Figure ''a'' was taken after the artificial fracture was created and figure ''b'' was taken after 4.5 h of hydraulic conductivity measurement (Bastiaens *et al.*, 2007).

With respect to healing, only indications of weak or partial healing have been observed for Boom Clay in the framework of the SELFRAC project: several of the artificially fractured samples showed some fracture cohesion after dismantling of the experiment. However, the cohesion was low and it was not possible to quantify it.

Based on these experimental results and the strong indication of laterally homogeneous deposition, De Craen *et al*. (2012) state that the existence of fissures that could result in a larger regional value of hydraulic conductivity of the saturated Boom Clay is highly improbable.

In the TIMODAZ experiments, the thermal impact on the self-sealing capacity of clay was investigated (Chen *et al*., 2010). The same phenomenon as in the permeameter test of SELFRAC has been observed at elevated temperatures in the TIMODAZ project, namely that an artificial fracture made in the Boom Clay sample quickly seals and is no longer discernible after the sample dismantling. Moreover, the technique µCT indeed showed the existence of pre-existing fissures in clay samples before testing. However, the permeability tests carried out independently in various laboratories by using different approaches on initially damaged, cut or sheared samples all provide a permeability value close to the initial permeability (Yu *et al*., 2010). This also holds for different pore water chemistry. This is a clear demonstration that fissures that are known to exist are not detected when running permeability tests. It is hence a confirmation of the excellent self-sealing behaviour of the Boom clay (Yu *et al*., 2010).

Huysmans (2006) investigated the effect of fractures on radionuclide transport in Boom Clay. She showed that fractures with properties similar to the fractures observed around previously excavated galleries in the Boom Clay have no significant effect on the radionuclide fluxes through the clay. From all fracture parameters, the extent of the fractured zone has the largest effect on radionuclide migration. The other fracture parameters including aperture, spacing and dip have a limited effect on the radionuclide fluxes. The limited extent of the fractured zone in the Boom Clay guarantees that the thickness of unfractured Boom Clay is large enough to limit the effect of the fractures.

3.4.2. Carbonate-rich layers with septarian carbonate concretions

The water outflow events during drilling of a number of boreholes around the PRACLAY gallery are summarized by Bastiaens *et al*. (2009). These water outflow events most likely originate from carbonate-rich layers containing septarian concretions.
The water outflow that occurred during drilling of borehole 2006/13 and probably also 2009/7 around the PRACLAY gallery of the HADES URF originated from septaria level S180 or S185. Because water-containing septarian concretions were reported previously in level S185, this is the most likely source. The amount of water was quite large (~0.4m³ for borehole 2006/13, ~0.8m³ for borehole 2009/7). Possible explanations are:

- The borehole reached a very large septarian concretion (most probably very long but rather thin). Assuming 20 % voids, such a concretion must have a dimension equivalent to ~2 m³ (2006/13), or ~4 m³ (2009/7). Note however, that these concretions are not spherical, bur elongated.
- For borehole 2006/13, because the inclination of the borehole is small (15°), the section of the borehole passing through the septaria level is long. Assuming S185 is 250 mm thick, the borehole inclination is 15° and the borehole diameter is 135 mm, about 1.5 m of the borehole passes through S185. Consequently, it is well possible that it passes through more than one septarian concretion (Figure 20).
- Several concretions are interconnected. This has already been observed in clay pits (Steendorp, level S20, De Craen, personal communication). At other locations, concretions of this particular level (S20) did not show this aspect. This means that,

although the occurrence of the individual septaria levels can be correlated over a large area, their aspect (size, degree of development, interconnection, …) can differ from one location to another.

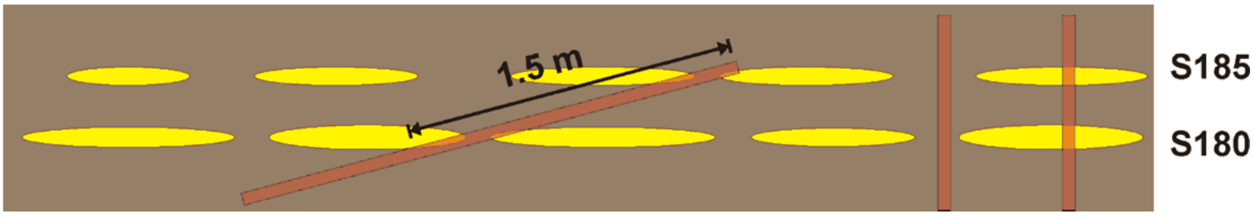

Figure 20: Schematical view of boreholes through septaria levels S180 and S185. Inclined boreholes have a higher possibility to encounter concretions than vertical boreholes.

It is highly unlikely that the water outflow was a result of a connection with the aquifers above the Boom Clay; at the location of the HADES URF, the top of the Boom Clay is located about 24 m above septaria level S185. The water originating from septaria layers is trapped in pockets. Inducing flow in these layers or mobilize/extract the water is almost impossible in natural conditions..

CONCLUSION: Experimental work has demonstrated that the swelling clay minerals and the visco-elasto-plastic behaviour of the Boom Clay seal fissures under saturated conditions and normal geomechanical stress. Several hypotheses have been formulated on the water outflow events, at present thought to be most likely originating from septarian concretions in the Boom Clay, observed during drilling events at the HADES URF. Currently, work is in progress on the distribution of septarian concretions in the Boom Clay in order to verify these hypotheses.

4. Discussion, Conclusions and knowledge gaps

This report gives a description of main transport processes occurring in Boom Clay both at the Mol site and at the regional scale. This report integrates evidence coming from different research areas (multiple lines of evidence), such as (1) large-scale experiments, (2) measured host rock properties of the Boom Clay, (3) the hydrogeological context of the Boom Clay and the surrounding aquifers and (4) experimental work on preferential flow.

With the current knowledge, these multiple lines of evidence all indicate diffusion–dominated transport through Boom Clay under past and present conditions or, at least, they do not give any evidence of the occurrence of other than diffusion-dominated transport. However, some unresolved issues still remain:

- Experimental evidence indicates that with the current knowledge, Onsagerian transport processes are most likely of minor relevance for solute transport in Boom Clay under current conditions.
- The shapes of the natural tracer profiles at Mol and Essen can be best explained by diffusion as the dominant transport process acting over geological time scales. However, the applied bottom boundary condition for the model, representing rapid flushing of the Oligocene aquifer, has not been supported by other evidence so far and thus remains speculative. Considering only diffusion gives good results in modelling the large-scale *in situ* experiment at the HADES URF.
- Results of the various lab-experiments and in-situ measurements at different scales (summarized in Yu *et al*., 2011) yielded consistent hydraulic conductivity values and indicate that Boom Clay at the Mol site has a very low hydraulic conductivity in general. The results finally demonstrate that the hydraulic conductivity of the Boom Clay, especially in the Putte and Terhagen Members, remains very consistent even for the relatively large geographical area of NE-Belgium. However, unexplained regional variations still exist today. From the experimentally measured host rock properties, it was found that the pores smaller than 25-30 nm are most likely to control the interconnectivity of the pore space in fine-grained samples of Boom Clay.
- Concerning the current hydrogeological context in NE-Belgium, we demonstrated that the hydraulic gradient over the Boom Clay at the Mol site is low and vertically downward oriented. On the regional scale, both upward and downward gradients exist, which can be considerably influenced by pumping. Very small vertical velocities were calculated in areas without groundwater extractions in the Oligocene aquifer. The regional Péclet numbers, calculated using the most adverse parameters, indicate a large variability over the study area. At some locations (outcrops, Campine cuesta) higher values (> 1) can be reached.
- Experimental and modelling work on preferential flow in Boom Clay has demonstrated that the swelling clay minerals and the visco-elasto-plastic behaviour of the Boom Clay seal fissures under saturated conditions and normal geomechanical stress. The existence of fissures that could result in a larger regional value of hydraulic conductivity of the saturated Boom clay is highly improbable. Several hypotheses have been formulated on the water outflow events most likely originating from septarian concretions in the Boom Clay, observed during drilling events at the HADES URF. However, more research is necessary on the septarian distribution in the Boom Clay in order to verify these hypotheses.

5. References

Aertsens M., Dierckx A., Put M., Moors H., Janssen K., Van Ravestyn L., Van Gompel Marc, Van Gompel Maria, De Cannière P., 2005a. Determination of the hydraulic conductivity, nR and the apparent diffusion coefficient on Ieper clay and Boom Clay cores from the Doel-1 and Doel-2b drillings. Restricted report of Belgian Nuclear Research Centre, SCK•CEN-R-3589, 285 p.

Aertsens M., Moors H., Van Ravestyn L., Van Gompel M., Van Gompel M., De Cannière P., e.a., 2005b. Determination of the hydraulic conductivity, the product ηR of the porosity η and the retardation factor R, and the apparent diffusion coefficient Dp on Boom Clay cores from the Mol-1 drilling. Restricted report of Belgian Nuclear Research Centre, SCK•CEN R-3503, 377 p.

Aertsens M., Maes N., Labat S., Van Gompel M., Maes T., 2010. Vertical distribution of HTO and 125I-transport parameters in Boom Clay in the Essen-1 borehole (Belgium). External report of Belgian Nuclear Research Centre, SCK•CEN-ER-67, 31 p.

Bastiaens W., Bernier F., Li X., 2007. SELFRAC: experiments and conclusions on fracturing, self-healing and self-sealing processes in clays: 2nd International meeting " Clays in Natural & Engineerd Barriers for Radioactive Waste Confinement , TOURS, France, 15-18 March 2005.- *In: Phys*ics and Chemistry of the Earth, 32:8-14(2007), p. 600-615.

Bastiaens, W., Van Marcke, Ph. and Li, X., 2009. Boreholes 2006/13 and 2009/7: observation and analyses of water outflow during drilling. Internal report of Belgian Nuclear Research Centre,SCK•CEN-I-2009.

Bear, J., 1972. Dynamics of Fluids in Porous Media. American Elsevier, New York.

Bernier F., Bastiaens W., Li X. L., 2004. Fractures and self-healing within the excavation disturbed zone in clays. European project SELFRAC: Fractures and self-Healing within the excavation disturbed zone in clays- Deliverable 4.

Bernier, F., Li, X.L., Bastiaens, W., Ortiz, L., Van Geet, M., Wouters, L., Frieg, B., Blümling, P., Desrues, J., Viaggiani, G., Coll, C., Chanchole, S., De Greef, V., Hamza, R., Malinsky, L., Vervoort, A., Vanbrabant, Y., Debecker, B., Verstraelen, J., Govaerts, A., Wevers, M., Labiouse, V., Escoffier, S., Mathier, J.F., Gastaldo, L., Bühler, Ch., 2007. Fractures and selfhealing within the excavation disturbed zone in clays (SELFRAC). Final report to EC (contract N°: FIKW-CT2001-00182), EUR 22585.

Brassines, S., 2007. Note on Onsagerian coupled transport phenomena. NIRAS/ONDRAF, Brussels, Belgium. 11p.

Chen G., Maes T., Vandervoort F., Xavier S., Van Marcke P., Honty M., 2010. Thermal impact on damaged argillaceous rocks: Permeameter test and Isostatic test on Boom Clay and Opalinus Clay from the TIMODAZ project. External Report of the Belgian Nuclear Research Centre, Mol, Belgium: SCK•CEN-ER-145, 42 p.

Mathier, J.F., Gastaldo, L., Bühler, Ch., 2007. Fractures and selfhealing within the excavation disturbed zone in clays (SELFRAC). Final report to EC (contract N°: FIKW-CT2001-00182), EUR 22585.

Databank Ondergrond Vlaanderen – peilfilters en peilmetingen – tabel opgemaakt 14/04/2011, op http://dov.vlaanderen.be

De Cannière, P., Moors, H., Lolivier, P., De Preter, P. and Put, M., 1996. Laboratory and *in situ* experiments in the Boom Clay. Final Report, EUR16927EN, European Commission. Nuclear Science and Technology, Luxembourg.

De Craen, M., Beerten, K., Honty, M. and Gedeon, M., 2012. Geo-scientific evidence to support the I2 isolation function (geology and long-term evolution) as part of the Safety and Feasibility case 1 (SFC1). External report of Belgian Nuclear Research Centre, SCK•CEN ER-184, 119 p.

de Marsily, G., 1986. Quantitative hydrogeology. Groundwater Hydrology for Engineers. Academic Press, San Diego.

Domenico, P.A., Schwarz, F.W. Physical and chemical hydrogeology, 2nd Edition. John Wiley and sons, New York, 1998.

Fetter C.W., 2001, Applied Hydrogeology (Fourth Edition), Prentice Hall, New Yersey.

Garavito, A. M., De Cannière, P., and Kooi, H., 2007. *In situ* chemical osmosis experiment in the Boom Clay at the Mol underground research laboratory. *Physics and Chemistry of the Earth, Parts A/B/C*, *32*(1-7), 421–433. doi:10.1016/j.pce.2006.01.004

Hemes S., Desbois G., Urai J., De Craen M., Honty M., 2012. Variability of the morphology of the pore space in Boom Clay from BIB-SEM, FIB and MIP investigations on representative samples. 2nd project report. External report of Belgian Nuclear Research Centre, SCK•CEN-ER-208, 65 p.

Horseman S.T., Higgo, J.J.W., Alexander J. and Harrigton J.F., 1996. Water, Gas and Solute Movement through Argillaceous Media. NEA report CC-96/1, 290pp.

Huysmans M., 2006. A geostatistical methodology for modelling groundwater flow and transport in low-permeability media: application on Boom Clay, Ieper Clay and Toarcian argillites. PhD thesis, K.U. Leuven, Belgium.

Huysmans M. and Dassargues A., 2005, Review of the use of Péclet numbers to determine the relative importance of advection and diffusion in low permeability environments, Hydrogeology Journal, 13(5-6), 895-904.

Jackson J.A. (Ed.), 1997. Glossary of geology (fourth edition). American Geological institute, Alexandria, Virginia, pp. 769.

Jeannée, N., Berckmans, A., Wouters, L., Deraisme, J. & Chilès, J. P. (2013). Quantifying the transferability of hydraulic parameters using geostatistics: The Boom Clay Case. *Physics and Chemistry of the Earth, Parts A/B/C*. doi:10.1016/j.pce.2013.05.014

Labat, S., 2011. Overview and analysis of 30 years piezometric observations in north-east Belgium. External report of Belgian Nuclear Research Centre, SCK•CEN -ER-163.

Labat S., Marivoet J., Wemaere I., Maes T., 2008a. Essen-1 borehole of the hydro/05neb campaign: technical aspects and hydrogeological investigations. External report of Belgian Nuclear Research Centre, SCK•CEN-ER-68.

Labat S., Wemaere I., Marivoet J., Maes T., 2008b. Herenthout-1 and Herenthout-2 borehole of the hydro/05neb campaign: technical aspects and hydrogeological investigations. External report of Belgian Nuclear Research Centre, SCK•CEN-ER-59.

Marivoet J., Jacques D., Van Geet M., Bastiaens W., Wemaere I., 2009. Considerations on upscaling of hydraulic and transport parameters for a plastic clay formation. External report of Belgian Nuclear Research Centre, SCK•CEN- ER-102.

Marivoet, J., Van Keer, I., Wemaere, I., Hardy, L, Pitsch, H., Beaucaire, C., Michelot, J.-L., Marlin, C., Philippot, A. C., Hassanizadeh, M., van Weert, F., 2000. A palaeohydrogeological study of the Mol site (PHYMOL project). Final report. European Commision. EUR 19146.

Mazurek M., Alt-Epping P., Bath A., Gimmi T., Waber H. N., Buschaert S., De Cannière P., De Craen M., Gautschi A., Savoye S., Vinsot A., Wemaere I., Wouters L., 2009. Natural Tracer Profiles Across Argillaceous Formations: the CLAYTRAC project. Nuclear Energy Agency, NEA No. 6253.

Mazurek M., Alt-Epping P., Bath A., Gimmi T., Waber H. N., Buschaert S., De Cannière P., De Craen M., Gautschi A., Savoye S., Vinsot A., Wemaere I., Wouters L., 2011. Natural tracer profiles across argillaceous formations. Applied Geochemistry, 26/7, 1035-1064.

Mertens J., Vandenberghe N., Wouters L. & Sintubin M. (2003) The origin and development of joints in the Boom Clay Formation (Rupelian) in Belgium. Geological Society, London, Special Publications, 216, 309-321.

ONDRAF/NIRAS, 2001. SAFIR 2: Safety Assessment and Feasibility Interim Report 2, NIROND 2001-06 E.

ONDRAF/NIRAS, 2009a. The ONDRAF/NIRAS Long-term Safety Strategy for the disposal of Radioactive Waste. SFC1 level 4 report, second full draft. NIROND-TR 2009-12E.

ONDRAF/NIRAS, 2009b. The Plan for the Safety and Feasibility Case 1. SFC1 level 4 report, first full draft. NIROND-TR 2009-13E.

ONDRAF/NIRAS, 2009c. The long-term safety assessment methodology for the geological disposal of radioactive waste. SFC1 level 4 report, second full draft. NIROND-TR 2009-14E.

Philippot, A.C., J.-L. Michelot and C. Marlin, 2000. A palaeohydrogeological study of the Mol site, Belgium (PHYMOL project). Rapport spécifique n°3: Analyse des isotopes et des gaz nobles. European Commision. Contrat N° FI4W-CT96-0026.

Soler, J. M., 2001. The effect of coupled transport phenomena in the Opalinus Clay and implications for radionuclide transport. *Journal of contaminant hydrology*, *53*(1-2), 63–84.

Vandenberghe, N. and De Craen, M., 2013. The Boom Clay: depositional area, present-day occurrence, stratigraphy and geology. External report of Belgian Nuclear Research Centre, SCK•CEN-ER-xxx. In preparation.

Vandenberghe, N., De Craen, M and L. Wouters. The Boom Clay Geology. From sedimentation to present-day occurrence. A review. In prep.

Vandersteen, K., Gedeon, M. and Rogiers, B., 2012. Transient model of the confined aquifers below the Boom Clay: 2011 update. External report of Belgian Nuclear Research Centre, SCK•CEN-ER-199, 132 p.

Vandersteen, K., Gedeon, M. and Leterme, B. Hydrogeology of North-East Belgium. Status report 2012. External report of Belgian Nuclear Research Centre, In preparation.

Volckaert G., L. Ortiz P. De Cannière, M. Put, S.T Horseman, J.F. Harrington, V. Fioravante, M. Impey, 1995. MEGAS: Modelling and experiments on gas migration in repository host rocks (Phase 1) - Final report. European Commission report, EUR 16235.

Weetjens E., Govaerts J., Aertsens M., 2011. Model and parameter validation based on *in situ* experiments in Boom Clay. External report of Belgian Nuclear Research Centre, SCK•CEN-ER-171, 46 p.

Wemaere I., Marivoet J., Beaufays R., Maes T., Labat S., 2002. Core manipulations and determination of hydraulic conductivities in the laboratory for the Mol-1 borehole (April-May 1997). Restricted report of Belgian Nuclear Research Centre SCK•CEN-R-3590.

Wemaere I., Marivoet J., Labat S., Maes T., Beaufays R., 2004a. Zoersel borehole of the hydro/96neb campaign: technical aspects and hydrogeological investigations. Geological disposal of conditioned high-level and long-lived radioactive waste. Restricted report of Belgian Nuclear Research Centre SCK•CEN-R-3892.

Wemaere I., Marivoet J., Labat S., Maes T., Beaufays R., 2004b. Rijkevorsel borehole of the hydro/96neb campaign: technical aspects and hydrogeological investigations. Geological disposal of conditioned high-level and long-lived radioactive waste. Restricted report of Belgian Nuclear Research Centre SCK•CEN-R-3930.

Wemaere I., Marivoet J., Labat S., Beaufays R., Maes T., 2005. The Weelde boreholes of the hydro/96neb campaign: technical aspects and hydrogeological investigations. Geological disposal of conditioned high-level and long-lived radioactive waste. Restricted report of Belgian Nuclear Research Centre, SCK•CEN- R-4187.

Wemaere I., Marivoet J., Labat S., 2008. Hydraulic conductivity variability of the Boom Clay in north-east Belgium based on four core drilled boreholes. *Physics* and Chemistry of the Earth 33, 24-36.

Yu, L., Gedeon, M., Wemaere, I., Marivoet, J. and De Craen M., 2011. Boom Clay Hydraulic Conductivity-a synthesis of 30 years of research. External report of Belgian Nuclear Research Centre, SCK•CEN-ER-122.

Yu, L., Rogiers, B., Gedeon, M., Marivoet, J., Craen, M. De, & Mallants, D., 2013. A critical review of laboratory and in-situ hydraulic conductivity measurements for the Boom Clay in Belgium. *Applied Clay Science*, *75-76*, 1–12. doi:10.1016/j.clay.2013.02.018.

Yu L., Weetjens E., Vietor T., Hart J.- *Integration of timodaz results within the safety case and recommendations for repostiory design (D14). Final report of WP6*.- Brussels, Belgium: European Commission, 2010.- 48 p.- (European Commission; TIMODAZ deliverable; EC FP6 TIMODAZ)

		Date	Approval
Author:	Katrijn Vandersteen	17/10/2013	
Verified by:	Eef Weetjens	17/10/2013	
QA-verification:	Elke Jacops	17/10/2013	
Approved by:	Mieke De Craen	21/10/2013	